CHANGES IN STABLE CARBON ISOTOPES OF METHANE ALONG A SALINITY GRADIENT IN A HYPERSALINE MICROBIAL MAT SYSTEM

A Thesis presented to the Faculty of the Graduate School at the University of Missouri-Columbia

In Partial Fulfillment of the Requirements for the Degree

Master of Science

By
ELYN POTTER

Dr. Cheryl Kelley, Thesis Advisor
MAY 2007

The undersigned, appointed by the dean of the Graduate School, have examined the thesis entitled

CHANGES IN STABLE CARBON ISOTOPES OF METHANE ALONG A SALINITY GRADIENT IN A HYPERSALINE MICROBIAL MAT SYSTEM

presented by Elyn Potter,

a candidate for the degree of Master of Science,

and hereby certify that, in their opinion, it is worthy of acceptance.

_____
Professor Cheryl Kelley

_____
Professor Mitchell Schulte

_____
Professor Keith Goyne

ACKNOWLEDGEMENTS

First and foremost, I would like to acknowledge my advisor, Dr. Cheryl Kelley. I am grateful to her for the opportunity to work on this project and for all of her help collecting data and for reading the many revisions of this thesis. I have really enjoyed our time working together! Many thanks to Dr. Brad Bebout, who collected samples and provided information about the saltworks and the microbial communities found there. I would like to thank my committee, Dr. Mitchell Schulte and Dr. Keith Goyne, for the constructive comments they made, as these greatly improved this paper. Thanks to Laura Lapham for her assistance in analyzing methane isotopes of my samples, and also for some interesting comments about the data. I thank the University of North Carolina at Chapel Hill for access to the IRMS located there. Thanks to Damon Bassett and Scott Lepley for helping with analyses in the MU stable isotope geochemistry lab. Jason Smith shared important information about the microbial community in these systems. One of the best aspects of working on this thesis was the opportunity to meet so many wonderful people; I am grateful to everyone I met during the course of this work for sharing so much of themselves with me. Thanks to the Exportadora de Sal de C. V. for allowing access to the study site. Financial support for this project was received from the NASA Exobiology program. Finally, I would also like to acknowledge the support of my friends and family. I could not have made it through school without their love and encouragement. In particular, I want to recognize my parents, my grandparents, my brothers, and my wonderful husband!

TABLE OF CONTENTS

LIST OF FIGURES

LIST OF TABLES

ABSTRACT

The purpose of this study was to examine how the stable carbon isotopes of methane and possible methanogenic substrates change in microbial mat communities as a function of salinity. Microbial mats were sampled from four different field sites located within the salterns of the Exportadora de Sal de C. V., Baja California Sur, Mexico. Salinities ranged from 50 to 106 parts per thousand (ppt) and samples were analyzed for the carbon isotopic composition of the dissolved inorganic carbon (DIC), mat material (particulate organic matter or POM) and methane. The POM samples were analyzed for their nitrogen isotopic composition as well. The POM $\delta^{13}C$ values ranged from -6.7 to -13.5‰, the DIC $\delta^{13}C$ values ranged between -1.4 and -9.6‰, and the $\delta^{15}N$ values of the POM ranged from -1.4 to 4.6 ‰. A. These values were similar to previously reported values. However, there are no prior reports of methane $\delta^{13}C$ values within the mats, and considerable variability among sites was found. The $\delta^{13}C$ values of methane range from -49.6 to -74.1 ‰; the methane most enriched in ^{13}C was obtained from the highest salinity pond. The apparent fractionation factors between methane and DIC, and methane and POM, in the mats were also determined and found to change with salinity. The apparent fractionation factors ranged from 1.042 to 1.077 when calculated from DIC, and from 1.038 to 1.068 when calculated from POM. The highest salinity pond showed the least fractionation, the moderate salinity pond showed the highest fractionation, and the low salinity sites showed fractionations that were in the middle of the other two sites. These differences in fractionation factors are most likely due to differences in the dominant methanogenic pathways at the different sites because of salinity differences.

1. INTRODUCTION

1.1 Significance of microbial mats

Photosynthetic microbial mats and stromatolites have a long history on Earth. Stromatolites are found in the fossil record from nearly 3.5 billion years ago, and persist into the present (Canfield and Des Marais, 1993). The abundance of stromatolites in the early fossil record is interpreted as evidence that these microbial communities were widespread on the Earth during the Precambrian (Walter, 1983). This makes microbial mats excellent candidates for study as proxies for early life on Earth (Des Marais et al., 2003).

Microbial mats are ecosystems that can exhibit chemical and population zonation on a millimeter or smaller scale in the vertical direction, yet can extend laterally for meters or kilometers. They may have had a dramatic impact on the chemistry of the atmosphere on the early Earth (Des Marais, 2003; Hoehler et al., 2001). For example, production and release of H_2 gas in microbial mats may have contributed to the net oxidation of the Earth's atmosphere (Hoehler et al., 2001).

Methane produced in microbial mats may have also played an important role in the Earth's atmosphere in the past. Solar luminosity was approximately 30% less when the solar system formed than it is today (Kasting, 2005). If the greenhouse effect in the Precambrian was the same as today, the decreased energy reaching the Earth would have resulted in global glaciation. However, there is no evidence for such a glacial episode prior to 2.3 billion years ago (Kasting, 2005). This situation has been dubbed the "faint

young sun paradox" (Pavlov et al., 2003). One possible solution to this paradox is elevated levels of atmospheric methane. Methane acts as a greenhouse gas; trapping of heat by methane in the atmosphere could have kept the temperature high enough to prevent global glaciation. The amount of methane present in the Proterozoic would largely have been controlled by methanogenic Archaea (Pavlov et al., 2003). The methane in the atmosphere would have been removed from the atmosphere at the onset of oxygenation of the atmosphere, and this could have triggered glaciation in the Paleoproterozoic (Kasting, 2005). Additionally, methane is a possible biosignature gas, which may be used to distinguish the activity of life on other planets (Bebout, 2002).

1.2 Hypersaline environments

As noted above, microbial mats and stromatolites have existed since the Precambrian and persist to the present day. Microbial mats were widespread in the Precambrian (Walter, 1983), but are more limited in extent in the marine realm in the modern Earth's oceans. The restriction in distribution of stromatolites in the Phanerozoic is thought to be due to the evolution of metazoans. Well developed mats are prevented from forming in most marine and freshwater settings because of the burrowing and grazing activity of metazoans (Garrett, 1970). Despite this, microbial mats can be found in a variety of places, including soils, lakes, streams, hot springs, and hypersaline waters (Des Marais, 1995).

Organisms from all three domains of life (Bacteria, Archaea, and Eukarya) are found in hypersaline environments (Oren, 2001). Because of the high extracellular salinity in these environments, special modifications to the chemical composition of the

cytoplasm of halophiles are required for survival. Biological membranes are permeable to water; if the solute concentration outside the cell is greater than inside it, the cell will lose water to the environment. To overcome this problem, most halophiles balance the osmotic pressure on their cells by maintaining high intracellular solute concentrations of either salts or organic solutes, such as glycerol or glycine betaine (Oren, 2001). Organic solutes do not require changes to cellular machinery, but they are energetically expensive. These organic solutes and their degradation products are important sources of carbon and energy to the microbial ecosystem (Oren, 1990). The other option for maintaining osmotic balance is to include a high concentration of salt (such as KCl) within the cell. This does not require as much energy as producing organic solutes, but does require special cellular adaptations (Oren, 2001).

There are many different metabolisms that can occur in hypersaline environments, despite the large proportion of energy that is expended by microorganisms in maintaining osmotic balance. The amount of energy produced by the different metabolisms has a direct impact on the highest salinity at which a given metabolic pathway will occur (Oren, 2002). According to Oren (2002), oxygenic respiration, oxygenic photosynthesis, and anoxic photosynthesis all persist up to salt saturation. Sulfate reducing bacteria can grow in salinities up to 240 ppt. Sulfide oxidation has also been observed at salinities of 240 ppt. Methanogenesis occurs at high salinities as well, with salinity tolerances of different methanogens ranging from 60 to 250 ppt depending on pathway.

The substrates that can be utilized by methanogenic archaea are limited in number, and each has a different salinity tolerance associated with it (Table 1).

Table 1. Salinity tolerances and carbon isotope fractionaton factors associated with different methanogenic substrates.

Substrate	Salinity tolerance [1]	Fractionation factor [2,3]
$CO_2 + H_2$	120 ppt	1.03 to 1.08
Acetate	60 ppt	1.01 to 1.03
Trimethylamine	250 ppt	1.05 to 1.07
Dimethylsulfide	No data	1.04 to 1.05
Methanol	250 ppt	1.07 to 1.09

[1] *Oren, 2002*
[2] *Conrad, 2005*
[3] *Whiticar, 1999*

The two most common methanogenic pathways in typical organic-rich marine and freshwater sediments are reduction of carbon dioxide with hydrogen gas (equation 1) and acetoclastic methanogenesis (equation 2; Conrad, 2005):

$$CO_2 + 4H_2 \rightarrow 2H_2O + CH_4 \quad (1)$$

$$CH_3COOH \rightarrow CO_2 + CH_4 \quad (2).$$

Generally, when sulfate is present in sediment pore water, these methanogenic pathways are suppressed because methanogens are outcompeted by sulfate reducers for H_2 and acetate, which are necessary substrates for both groups. This is because sulfate reduction is thermodynamically and kinetically more favorable than methanogenesis (King et al., 1983). However, there are some methanogens that can also use noncompetitive substrates and are thus able to coexist with the sulfate reducers. Noncompetitive

substrates include methylated compounds (other than acetate) such as dimethylsulfide (equation 3; van Leerdam et al., 2006), methylated amines (example—trimethylamine; equation 4; Oren, 2001), or methanol (equation 5; Oren, 2001):

$$2\ CH_3SCH_3 + 3\ H_2O \rightarrow 3\ CH_4 + HCO_3^- + 2\ H_2S + H^+ \quad (3)$$

$$4\ (CH_3)_3N + 9\ H_2O + H^+ \rightarrow 9\ CH_4 + 3\ HCO_3^- + 4\ NH_4^+ \quad (4)$$

$$4\ CH_3OH \rightarrow 3\ CH_4 + HCO_3^- + H_2O + H^+ \quad (5).$$

In hypersaline environments, methane is typically produced from noncompetitive substrates (Conrad, 2005). Methylated amines are present in hypersaline environments as degradation products of glycine betaine, which is a compound used by halotolerant and halophilic organisms as an osmoregulant (Oren, 1990). Dimethyl sulfide (DMS) in marine settings is commonly a breakdown product of dimethylsulfionopropionate (DMSP); however, DMS in hypersaline environments has been shown to be a product of reactions between biologically produced hydrogen sulfide and low molecular weight organic compounds (Visscher et al., 2003). Methanol in these environments is derived from microbial degradation of pectin (Conrad, 2005).

1.3 Stable isotopes

1.3.1 Stable carbon isotopes

Carbon is one of the most abundant elements in the universe, and is essential for life on Earth. There are two stable isotopes of carbon; ^{12}C makes up 98.89% of carbon on Earth, while ^{13}C accounts for 1.11 %. The stable isotopic composition of carbon is

expressed using delta notation. Delta notation for carbon is written as $\delta^{13}C$ and is calculated as in equation 6 (Faure, 1986):

$$\delta^{13}C \text{ (in permil)} = ((R_{sample} - R_{standard})/R_{standard})*1000, \quad (6)$$

where R is the ratio of $^{13}C/^{12}C$. The standard most commonly used for carbon isotope notation is Pee Dee Belemnite (PDB), which is a carbonate fossil from the Cretaceous. The value of the $^{13}C/^{12}C$ for this standard is 0.0112372 ± 0.0000029 (Craig, 1957). Another term frequently used in stable isotope discussions is α, or the fractionation factor. This is calculated using equation 7 (Conrad, 2005):

$$\alpha = (\delta^{13}C_A + 1000)/(\delta^{13}C_B + 1000), \quad (7)$$

where $\delta^{13}C_A$ is the isotopic composition of the reactant and $\delta^{13}C_B$ is the composition of the product. The fractionation factor is a measure of how offset the isotopic value of the product is from the substrate from which it was formed. In the case of methanogenesis, $\delta^{13}C_A$ is the isotopic composition of the methanogenic substrate and $\delta^{13}C_B$ is composition of the methane produced. The term fractionation factor is reserved for methanogenesis from only one substrate. In measurements of methane produced in environmental samples, methane is generally being produced from a combination of two or more substrates. For this reason, the term apparent fractionation factor is used rather than fractionation factor in this thesis.

Stable carbon isotopes of methane can be used to identify different sources of methane, since biogenic methane is typically very depleted in ^{13}C relative to methane from other sources (Whiticar, 1999). Individual measurements of the isotopic composition of biogenic methane can range from -110‰ to -50‰ (Whiticar, 1999). This is because each methanogenic pathway has a different isotopic fractionation factor associated with it (Table 1), and the substrate from which the methane is formed will have an effect on the isotopic composition of the methane. Comparing the apparent fractionation factor observed in the environment with fractionation factors measured from individual substrates can help determine the relative proportions of the substrates being used by methanogens in that environment. Carbon isotope fractionation during methanogenesis from carbon dioxide is also affected by temperature (Equation 8, Blair et al., 1993):

$$\ln \alpha_{CO2} = 23.0/T - 0.022, \quad (8)$$

where T is the temperature in Kelvin, and α_{CO2} is the fractionation factor associated with methanogenesis from reduction of carbon dioxide. Unfortunately, the temperature dependence of other methanogenic substrates has not been established. There are additional factors that affect the fractionation factor of methanogens. These include rates of methane production, growth phase of a given microbial culture, species of methanogen, and hydrogen gas availability (Conrad 2005).

1.3.2 Stable nitrogen isotopes

There are two stable isotopes of nitrogen in the environment; ^{14}N makes up about 99.64% of nitrogen in the atmosphere, while ^{15}N accounts for 0.36% (Hoefs, 2004). The isotopic composition of nitrogen is expressed using delta notation (as for carbon) using equation 9 (Faure, 1986):

$$\delta^{15}N = ((R_{sample} - R_{standard})/R_{standard})*1000, \quad (9)$$

where R is the ratio of $^{15}N/^{14}N$. The standard used for nitrogen is N_2 in air, which has a $^{15}N/^{14}N$ ratio of 0.0036765 ± 0.00000081 (Junk and Svec, 1958).

Nitrogen isotopes vary widely in nature. Values of $\delta^{15}N$ range from -50 to +50‰, with most values falling into the -20 to +20‰ range (Hoefs, 2004). Nitrogen fixation typically yields organic matter with $\delta^{15}N$ values between -1 and +3‰ (Fogel and Cifuentes, 1993). In general, $\delta^{15}N$ values increase with increasing recycling of particulate nitrogen, with approximately a 3‰ increase per trophic level (Minawaga and Wada, 1984). This means that the relative age of organic matter can be determined using $\delta^{15}N$. For example, organic matter in the ocean results shows an increase of $\delta^{15}N$ with depth in the oceans because organic particles that have been in the ocean longer have been subject to greater degrees of bacterial degradation (Faure, 1986).

Nitrogen content in sediments is typically linked to carbon abundance, because nitrogen is generally associated with organic matter (Faure, 1986). In the oceans, carbon to nitrogen ratio (C/N) increases with depth, because nitrogen is selectively removed by biological degradation of organic matter (Faure, 1986).

1.4 Aim of the thesis

The purpose of this thesis is to examine how the isotopic composition of methane produced in microbial mats in the salterns of the Exportadora de Sal de C. V., Baja California Sur, Mexico changes along a salinity gradient. Mat samples from each of four different salinities were analyzed for the stable carbon isotopic composition of their particulate organic material (POM), dissolved inorganic carbon (DIC), and methane. These different carbon pools were measured in an attempt to characterize the isotopic fractionation between methane and potential substrate, and in this manner to determine the relative importance of the different methanogenic pathways at each site. Calculations of the apparent fractionation factors of methane in each field site were made and compared to known fractionation factors to accomplish this. The stable nitrogen isotopic composition and carbon and nitrogen content were also measured. This was done in order gather supporting data from these mat systems, and to attempt to understand nitrogen cycling in the system.

2. STUDY SITE

2.1 Description of sample locations

The study sites are located in the salterns of the Exportadora de Sal in Guerrero Negro, Baja California Sur, Mexico (Figure 1). The town of Guerrero Negro is situated in the San Vizcaino Desert immediately south of the border between Baja California and Baja California Sur near the Ojo de Liebra Lagoon. The Exportadora de Sal pumps water from the Ojo de Liebra Lagoon, which has a salinity of approximately 40 ppt (Bebout et al., 2002), into a system of 14 evaporation ponds where it becomes progressively more saline (Table 2). These shallow (averaging less than 1 m) evaporating basins cover an area of more than 250 km^2 (Des Marais et al., 1989). Water flows through the evaporation ponds and thence into crystallization ponds where halite is deposited and collected by the salt company.

These evaporation ponds have been studied extensively over the last 20 years (Des Marais et al., 1989), particularly Ponds 4 and 5 (Des Marais and Canfield, 1994; Des Marais, 1995; Bebout et al., 2002; Bebout et al., 2004; Kelley et al., 2006). The concentration ponds with salinities between 50 and 130 ppt have cohesive, well developed microbial mats. The mats of interest for this study are submerged year round and range in thickness between 1 to 10 centimeters (Des Marais, 1995). The mats have sub-millimeter to millimeter laminations showing wide variety of colors from the different communities of microorganisms inhabiting different depths within the mat.

Despite the small vertical scale of these mats, they cover an area of approximately 100 km^2 (Des Marais et al., 1989).

Table 2. Salinity measured at the field sites in December 2005, temperature measurements taken in December 2005, and yearly averages of long term salinity data ranging from 1990 to 1998.

Site	Salinity, ppt December 2005	Temperature, °C December 2005	Salinity range[1], ppt
Natural marsh	50	19	no data
Pond 1	55	20	30 to 50
Pond 4	90	16	65 to 96
Pond 6	106	19.5	112 to 143

[1]*Shumilin et al, 2002.*

The mats are mainly composed of microorganisms and mucilage with a small (less than 5%) amount of sediment. Cyanobacteria (predominantly *Microcoleus*) dominate in the upper 2 mm of the mat (Ley et al, 2006).

2.2 Biogeochemical cycling in hypersaline microbial mats in the salterns of Exportadora de Sal de C.V.

Microbial mats are complex ecosystems where nutrients are cycled very rapidly. The organisms within mats live in close proximity; end products of many metabolisms are the required substrates of others (Bebout et al., 2002). In the mats of the Guerrero Negro system, there are sharp chemical gradients of oxygen, hydrogen gas, hydrogen sulfide (ΣH_2S) and other compounds (Garcia-Pichel et al., 1994). The primary carbon

fixation process in these mats is photosynthesis (both oxygenic and anoxygenic). Oxygen is produced through photosynthesis at the surface of the mat during the day and penetrates the mat to a depth of approximately 2 mm (Des Marais, 2003). Due to high rates of photosynthesis, oxygen in the mat can reach a concentration up to five times as high as air saturated seawater (Des Marais, 1995). At night, the oxygen produced during the day is consumed by respiration (Des Marais, 1995), and the entire mat becomes anoxic (Canfield and Des Marais, 1991).These changing conditions and sharp chemical gradients mean that there are many different metabolic niches available to microorganisms (Garcia-Pichel, 1994).

Sulfur within the mat is cycled by dissimilatory sulfate reduction and sulfur oxidation (Canfield and Des Marais, 1991). Hydrogen sulfide is found in the mat pore waters in the anoxic regions; the oxygen-sulfide interface migrates up and down within the mat over the course of a diel cycle (Des Marais, 1995). Sulfate reduction occurs in the aerobic zone as well as the anaerobic zone within these mats (Canfield and Des Marais, 1991). With the exception of aerobic sulfate reduction, these processes are typical in most aquatic ecosystems. However, in microbial mats, microbial and chemical zonation occurs on scales of a millimeter or less (Canfield and Des Marais, 1993).

Nitrogen in the mat is supplied by nitrogen fixation, as well as diffusion from the overlying water and remobilization of organic nitrogen from within the mat (Des Marais, 1995). The most important of these sources of nitrogen to the mat is probably organic matter within the mat (Des Marais, 1995). Rates of nitrogen fixation within the mat are controlled by a diel cycle as well; since nitrogen fixation is inhibited by oxygen, nitrogen fixation occurs primarily at night (Des Marais, 1995).

Methanogenesis has also been observed within these hypersaline mats (Hoehler et al., 2001; Bebout et al., 2002; Kelley et al., 2006). As has been previously mentioned, methanogenesis via carbon dioxide reduction or acetatoclastic methanogenesis is inhibited by the presence of sulfate. Manipulations of mat communities in a greenhouse facility maintained at NASA Ames Research Center showed that reducing sulfate concentrations increases methane production (Bebout et al., 2004). This implies that there are acetoclastic or hydrogenotrophic methanogens present in these salterns, though they may not account for a significant proportion of the methane produced under *in situ* conditions (Smith et al., 2007). Hydrogenotrophic methanogens may be able to coexist with sulfate reducing bacteria due to the large amounts of H_2 contained in the surface of the microbial mats (Hoehler et al., 2002).

3. METHODS

3.1 Sampling methods

Mats were sampled in December 2005 from the Exportadora de Sal de C. V. from four sites with four different salinities. Pond 1 has a salinity of 55 ppt, Pond 4 has a salinity of 90 ppt, Pond 6 has a salinity of 106 ppt, and the marsh has a salinity of 50 ppt (Table 2). Mats were sampled from an area in each site that is representative of the mats located in that site. The salinity of each site was measured using a refractometer prior to sampling, and methane production and concentration within the mats were measured (B. M. Bebout, unpublished data; Figures 2 and 3). Cores of the mats were taken using a 60 ml syringe with the needle end cut off. The cores were then extruded from the syringe so that slices of the mat could be sampled. Three depth intervals were obtained from all cores: 0 to 4 mm, 10 to 14 mm, and 26 to 30 mm. Samples taken for analysis of particulate organic matter and dissolved inorganic carbon required one slice each. Since concentrations of methane were expected to be low (Bebout et al., 2002), two core slices per sample were obtained for methane samples analyses to ensure that the amount of methane present in the sample was above the analytical detection limits of the Isotope Ratio Mass Spectrometer (IRMS). Triplicate samples were taken from each site for all three parameters. Care was taken during the collection of the mat to sample quickly in order to minimize exposure to air.

Mat samples from the NASA Ames Research Center greenhouse facility were also sampled for analysis of dissolved inorganic carbon and methane carbon isotopes.

These mats were taken from Pond 4 in December 2005 and transported from Guerrero Negro to the NASA Ames Research Center in Moffett Field, California, where they are maintained in flow boxes. The sampling method and flow box set up has been previously described (Bebout et al., 2002; Bebout et al., 2004). In brief, mat samples were collected from Pond 4 by divers and put into tight fitting black opaque boxes to minimize exposure of the anoxic layers of the mat to light and air. The mats were covered in water with a salinity of 130 ppt overnight to slow metabolic rates. They were then drained and transported to California covered in plastic film to keep them moist. At the greenhouse facility, the boxes containing the mats were installed into the flow box table and covered with brine that has approximately the same composition as the brine at the field site. These mats were maintained in the NASA Ames greenhouse facility for approximately two months, and then sampled in February 2006.

The first purpose of sampling the greenhouse mats was to determine if the methane in the greenhouse mats was different than in Pond 4 and therefore whether moving the mats from Guerrero Negro to NASA Ames or the artificial environment had altered the methanogenic community. The second reason for sampling the greenhouse mats was to determine if sampling different amounts of mat material had an effect on the methane isotopes. As previously mentioned, two cores of each interval were taken at the field sites in the Exportadora de Sal de C. V. for analysis of the carbon isotopic composition of methane. After the first slice of mat material was added to the sample vial, there was a period of approximately five minutes when the sample vial was open to the atmosphere. Because methane is not very soluble in water (Wiesenburg and Guinasso, 1979), methane could have escaped during sampling. Methane diffusion and

loss to the atmosphere could have fractionated the methane originally present in the sample so that the isotopic composition of the remaining methane was altered. Therefore, it was necessary to determine if the isotopic composition of the methane was different in samples of one core (sampling method where vials were immediately capped after insertion of the mat slice) and samples of two cores (where the vial headspaces were flushed with nitrogen gas, but open to the atmosphere for approximately 5 minutes). Since all the samples from the field site were sampled using two cores, it was important to verify that the sampling protocol in the field did not compromise the isotopic composition of the methane measured from those sites.

3.2 Analytical methods

3.2.1 Dissolved inorganic carbon (DIC)

The stable carbon isotopic composition and concentration of DIC were measured in Ponds 1, 4, 6, the natural marsh, and the greenhouse mats. Samples for DIC were centrifuged in a perforated cylinder with filter paper at the bottom for five minutes in order to separate the pore water from the mat. The volume of the pore water was recorded, and the water was injected via syringe into evacuated 2 ml serum vials with crimped on rubber stoppers. The vials were frozen and stored upside down to help prevent gas diffusion across the stopper. In preparation for analysis, 1000 µl of 5M H_3PO_4 was added to each 2 ml serum vial. This acidified the samples to ensure that all present CO_2 entered the gas phase. The samples were shaken to help gas escape into the headspace. Helium gas was also added to increase pressure inside the vials to atmospheric pressure. The volume of helium gas injected into the vials was calculated

using equation 10:

$$\text{Volume}_{He} = 1000 - \text{Volume}_{sample} \quad (10)$$

where Volume_{He} is the Volume of helium in microliters (μl), and Volume_{sample} is the volume of the pore water extracted from the mat in microliters (μl). The approximate volume of gas needed for isotopic analysis was estimated using previously reported amounts of DIC from within the pore water (Kelley et al., 2006). DIC samples were injected into a Hewlett Packard gas chromatograph (GC) connected via a GC Combustion III interface to a ThermoQuest Finnigan Delta Plus XL isotope ratio mass spectrometer (IRMS) for analysis.

The concentration of DIC in each sample was determined from the chromatogram. The mean peak area per mole of carbon dioxide in the standard injection measured by the IRMS was calculated, then this value was multiplied by the peak area of each sample to give the number of moles of carbon dioxide in the sample. The concentration (in millimolar) of each sample was then calculated using the following equation:

$$(N/V_1)*(V_2/V_3)*10^6 \quad (11)$$

where N is the amount of CO_2 (in millimoles) in the sample, V_1 is the volume of pore water (in microliters) extracted from the mat, V_2 is the volume of helium gas (in microliters) added to the sample vials, and V_3 is the volume of gas (in microliters)

injected into the GC.

3.2.2 Particulate organic material (POM)

Measurements of the isotopic composition and percentages of carbon and nitrogen of the POM were taken from Ponds 1, 4, 6, and the natural marsh. Samples for POM carbon and nitrogen isotopes were cored, sliced, and refrigerated in scintillation vials. The samples were prepared for analysis using the method described by Hedges and Stern (1983). The mat material was dried in a drying oven at 60 ºC for approximately one week. The samples were homogenized with an agate mortar and pestle and acidified to remove carbonate by adding approximately 2 ml of 1.2 M HCl was added to each sample. Samples were left to react overnight; subsequent additions of acid were required for some samples if carbonate was still visible in the sample after this time period. After acidification and drying, samples were homogenized a second time with the agate mortar and pestle. Samples were weighed before and after acidification in order to determine the mass change from salts created by the acidification and drying process. Normalization to the original sample mass was not necessary for isotopic analyses, but it was needed for the analyses of %C and %N within the samples. The homogenized samples were weighed into tin boats and flash combusted in a Carlo Erba NA 1500 Elemental Analyzer (EA) and then analyzed on the ThermoQuest Finnigan Delta Plus XL IRMS using a Conflow III interface. Measurements of %C, %N, $\delta^{13}C$ and $\delta^{15}N$ were made in this manner.

3.2.3 Methane

Measurements of methane stable carbon isotopic composition were taken from Ponds 1, 4, 6, the natural marsh, and the greenhouse mats. The greenhouse mats were

sampled twice; one set of samples contained slices from two mat cores and one set contained slices from one core. First 10 ml of 0.55 M potassium hydroxide was added to 50 ml serum vials. Potassium hydroxide is used to stop any metabolic activity and to ensure that the DIC within the pore water remained in the aqueous phase once the sample was added. The headspaces of the vials were then flushed with N_2 gas until sample addition. The headspaces in the vials were flushed with N_2 again, stopped with solid butyl rubber stoppers and crimped closed. The samples were refrigerated upside down until analysis to prevent communication with the atmosphere.

To begin analysis, two syringes were used to recover gas from the headspace of the vial; one injected water into the vial in order to force gas into the second. The syringes were left in place for a few minutes after this procedure to ensure that no fractionation occurred across the small hole of the needle. The samples were injected into a He carrier line that passed through a liquid N_2 and ethanol cryofocusing trap and a second liquid N_2 trap following a method described by Rice et al. (2001). The purpose of these traps was to concentrate the methane, as well as to remove any CO_2 or water present in the sample. The samples were analyzed using a FinniganMat 252 IRMS (Thermofinnigan, Bremen, Germany) with a Finnigan ConFlo interface, modified after Brenna et al. (1997) and a 5890 Hewlett Packard Gas Chromatograph.

3.3 Statistical analysis

An F-test followed by a t-test was used to determine whether the means of the samples taken from the different ponds were equivalent. These were performed using the Data Analysis package in Microsoft Excel. Both of these tests are based on modifications of the normal distribution. These tests operate by using the concept of the null hypothesis which states that the treatment (in this case the different salinities) has no effect. The F-test is used to determine whether the variances of two sample sets are the same (Davis, 1986). The null hypothesis in the F-test states that the variances of two sets of data are equal. The results of the F-test determine whether it is more appropriate to use a t-test for samples with equal variance or unequal variances. The t-test is used to establish the likelihood that one data set is equivalent to another (Davis, 1986). The t-test is the statistical test typically applied to data sets with small numbers of samples in order to account for the increased uncertainty introduced by using smaller sample sets (Davis, 1986). The null hypothesis for the t-test states that the means of the sets of samples are equal. The confidence level (α) in statistical testing is the likelihood that the null hypothesis will be rejected even though it is correct (type I error). Microsoft Excel returns a P-value for both F- and t-tests. A P-value is the likelihood that the difference between groups is due to randomness of the sample (Whitley, 2002). If the P-value is less than the confidence level, the null hypothesis is rejected and the means or variances are not equal. If the P-value is greater than the confidence level, the null hypothesis is not rejected. A confidence level of 0.05 was chosen for the t-tests and F-tests, which means that there is a 5% chance that the means or variances of the data will be incorrectly interpreted as not equal.

Analysis of variance, or ANOVA, was also used to analyze data sets. This statistical test was also performed using the Data Analysis package in Microsoft Excel. A two-way ANOVA is useful to determine which of two variables has more variance associated with it (Davis, 1986). For a two-way ANOVA, there are two null hypotheses; in this study, the null hypotheses were that 1) the means of the different depth intervals samples were the same and 2) that the means of the different ponds were equal. For the two-way ANOVAs, a confidence level of 0.05 was used.

4. RESULTS

4.1 Dissolved organic matter

The $\delta^{13}C$ values of DIC from the greenhouse mats, sampled in February 2006, ranged from -5.5 ± 0.1 to -3.5 ± 0.5‰, while samples obtained in the field from Pond 4 in December 2005 ranged in isotopic composition from -4.9 ± 0.5 to -1.4 ± 1.1‰ (Figure 4). An F-test shows that the variances of these two groups are equal ($p > 0.05$), and although there is about a 4‰ difference in $\delta^{13}C$ values in the surface interval, a t-test between these two sets of data showed that the means were equal as well ($p > 0.05$).

Stable carbon isotopic values of DIC (Figure 5) measured from mats growing *in situ* ranged from -1.4 ± 1.1 to -9.6 ± 0.7‰. A two-way ANOVA showed that there were significant differences between the means of the DIC in the different field sites ($p < 0.05$), but no significant change in mean isotopic composition with depth within the mat ($p > 0.05$). Pond 6, which had the highest salinity, has the most negative DIC $\delta^{13}C$ values. The $\delta^{13}C$ values of DIC from the greenhouse mats are similar to previously reported values from these mats (Kelley et al., 2006), and DIC from the mats that were sampled *in situ* have isotopic values that also show agreement with previous reports (Des Marais et al., 1989).

The DIC concentration (Figure 6) in the *in situ* mats ranged from 1.7 ± 1.0 to 8.5 ± 1.0 mM. A t-test showed that the means of the DIC concentration in the greenhouse and Pond 4 mats were equal ($p > 0.05$; Figure 7). In general, the concentration of DIC increases with depth, although in Pond 6 it decreases slightly in the deepest interval. All

of the sites had fairly similar DIC concentrations.

4.2 Particulate organic matter

Analyses of the $\delta^{13}C$ values of POM, shown in Figure 8, ranged from -6.7 ± 0.5 to -13.5 ± 0.3‰, with the mat material of Pond 1 being more enriched in ^{13}C than the other ponds. A two-way ANOVA showed that the mean $\delta^{13}C$ values of the POM were significantly different between ponds in the field ($p < 0.05$), but there was no significant change in the mean isotopic composition with depth ($p > 0.05$). There was agreement with previous reports of the values of POM isotopic composition (Kelley et al., 2006; DesMarais et al., 1989).

The $\delta^{15}N$ values of the mat material (Figure 9) ranged from -1.4 ± 0.3 to 4.6 ± 0.5‰. A two-way ANOVA showed that the depth intervals were the same ($p > 0.05$), but the ponds were different from each other ($p < 0.05$).

The carbon to nitrogen ratio increases with depth in the mat in each field site (Figure 10). The C/N ratios range from 6.6 ± 2.0 to 12.6 ± 0.9, with the lowest ratios occurring in the surface intervals and the ratio increasing with depth. A comparison of %C to %N within the mat shows that the mat material is closest to Redfield ratio (6.625, Redfield et al., 1963) at the surface. The Redfield ratio is the average stoichiometric ratio of carbon to nitrogen of marine phytoplankton. The ratio increases with depth, which indicates that the mat material has been subjected to increasing degrees of microbial degradation with depth.

4.3 Methane

Methane measured from both one and two core slices (Figure 11) sampled in the greenhouse ranged in isotopic composition from -68.8 ± 7.0 to -62.5 ± 6.8‰. The carbon isotopic composition of methane from mats sampled in the field from Pond 4 ranged from -74.1 ± 0.9 to -72.6 ± 0.9‰ and is also shown in Figure 11. A t-test performed on the greenhouse mat data between those that were sampled using one core and those using two showed that the means of these two groups were equal. The results of t-tests between the greenhouse data and the Pond 4 data showed that the methane isotopic composition was significantly different between these two sample sites.

There was a very wide range of methane carbon isotopic values in the mats sampled *in situ*; values ranged from -49.6 ± 1.5 to -74.1 ± 0.9‰ (Figure 12). A two-way ANOVA showed that the ponds were statistically different from each other, but there was not a significant difference between the depth intervals that were sampled. The lack of change with depth of the isotopic composition of the methane in the ponds may be because samples were only taken from the upper three centimeters of the mat. There may be changes in the carbon isotopic composition of methane deeper in the mat, or in the sediments underlying the mat. It is also possible that the lack of change with depth of the methane isotopes is that only three depth intervals were sampled. In a microbial mat, where sharp chemical gradients occur in small depth intervals, it may be possible that the methane isotopic composition also changes on very small scales that were not detected. Pond 6 had the highest $\delta^{13}C$ values, while the most negative $\delta^{13}C$ values were measured in Pond 4.

5. DISCUSSION

5.1 Comparison of Pond 4 mats to greenhouse mats

The samples from the greenhouse that had different amounts of mat material (i. e. one core slice or two core slices) had methane carbon isotopic compositions that were statistically the same. Therefore the amount of mat material used had a negligible effect on the measurements of the isotopes. This shows that the extra time taken sampling two cores in the field sampling procedure did not alter the carbon isotopic composition of the methane in the field sites.

The measurements of methane taken from the greenhouse and Pond 4 mats had mean values of isotopic composition and concentration that were statistically the same. These greenhouse mats were originally taken from Pond 4, but the mats in the greenhouse facility had been transported and maintained under controlled conditions for approximately three months. The discrepancy between methane isotopes from these Pond 4 and the greenhouse could mean that the methanogens have been affected by the transport or artificial conditions in the greenhouse.

The isotopic composition of the DIC is statistically the same in the greenhouse mats and the *in situ* Pond 4 mats (Figure 4). The DIC concentration is also statistically the same in Pond 4 and the greenhouse mats, and both mats show very similar trends, with concentration of DIC increasing with depth (Figure 7). The DIC isotopic composition and concentration is primarily controlled by carbon fixation, remineralization, and diffusion from overlying water (Des Marais and Canfield, 1994).

Methane concentrations measured in mats from different sites ranged from less than 1 to 22 μM (B. M. Bebout, unpublished data, Figure 3). This is between 2 and 5 orders of magnitude less than DIC concentrations (Figure 6). In addition to the concentration differences between methane and DIC within these mats, methanogenesis accounts for less than 0.4% of the carbon flux out of these mats (Bebout et al., 2004), so methanogenesis is not likely to have a significant impact on the DIC isotopic composition.

5.2 Particulate organic matter

The carbon to nitrogen ratio of the particulate organic matter within the mats sampled *in situ* increases with depth (Figure 11). This is consistent with high photosynthetic rates at the top of the mat and increasing heterotrophy with depth within the mat. The selective removal of nitrogen relative to carbon in deeper layers in the mat is consistent with observations that nitrogen from recycling of organic material is the primary source of fixed nitrogen within the mat (Des Marais, 1995).

The POM data show Pond 1 to be a bit different than the other sites. In each pond except Pond 1, $\delta^{15}N$ values within the mat increase with depth (Figure 9). In general, biological degradation selectively removes ^{14}N relative to ^{15}N (Faure, 1986). Therefore, it seems that the nitrogen in deeper levels of the mat has been subject to more degradation, possibly because the organic matter at the bottom of the mat is older than the organic matter at the top. This observation seems to be best explained by new photosynthate at the mat surface, possibly containing newly fixed nitrogen. In Pond 1, the nitrogen isotopic trend is reversed and the $\delta^{15}N$ values decrease with depth in the mat

(Figure 9). Pond 1 is the site with the least negative $\delta^{13}C$ values (Figure 8), particularly at the surface. The surface interval of Pond 1 mat also has the highest percentage of carbon and nitrogen (and therefore the most organic matter) of all of the samples. The isotopic trends and the carbon and nitrogen content of the mat probably reflect high rates of productivity in Pond 1; if productivity is high enough to locally deplete DIC and nitrogen, the fractionation factors associated with these may not be expressed as fully as it is in the other sites, resulting in a decrease in $\delta^{13}C$ and $\delta^{15}N$ values at the surface of the mat.

In a previous study, the difference between the DIC $\delta^{13}C$ values and the POM $\delta^{13}C$ values was found to be approximately 7‰ in ponds with salinities between 90 and 108 ppt due to high photosynthetic rates and sulfide oxidation (Des Marais et al., 1989). The difference between these two values in this study was similar in the deeper intervals of the mat in Ponds 1, 4 and the marsh (Figure 13). The difference between DIC $\delta^{13}C$ values and the POM $\delta^{13}C$ values at the mat surface is much greater in Pond 4 and much less in Pond 1. This may be due to a difference in photosynthetic rates at these two sites. In Pond 6, the difference in these two isotopic measurements is low compared to the other sites. This pond has a similar salinity to its previously reported multi-year average (Shumulin et al., 2002), so one might expect them to have a similar DIC-POM offset. One possible explanation is a breach in the barrier between Pond 6 and Pond 11 that occurred in August, 2005 that temporarily introduced higher salinity water into Pond 6 (B. M. Bebout, pers. comm.). This may have disrupted the microbial communities enough to change the isotopic composition of the DIC or POM or both.

5.3 Apparent fractionation factors associated with methanogenesis in the mats sampled *in situ*

Examining the fractionation factor (α) associated with methanogenesis at each site is a useful way to analyze stable isotopic data, because it gives a measure of how offset the methane isotopic value is (in ‰) from the substrate from which it is formed. A true fractionation factor would be the isotopic offset expected from a known substrate, which might be measured in a pure culture. In this case, since it is likely that more than one substrate is being used, apparent fractionation factors are reported (Table 3).

Table 3. Apparent fractionation factors of methane at each site calculated from dissolved inorganic carbon (DIC) and particulate organic matter (POM).

Site	DIC	POM
Marsh	1.058 to 1.062	1.051 to 1.056
Pond 1	1.054 to 1.059	1.049 to 1.052
Pond 4	1.074 to 1.077	1.067 to 1.068
Pond 6	1.042 to 1.045	1.038 to 1.042

The fractionation factor is calculated using Equation 2. The $\delta^{13}C$ values of methane plotted against the $\delta^{13}C$ values of the DIC are shown in Figure 14, with the lines representing equal α values. Pond 1 and the natural marsh, which are the lowest salinity sites, have similar apparent α values. Pond 4 has the highest apparent α value, and Pond 6, which is the highest salinity pond has the lowest α value. Based on these observations of the apparent fractionation, it appears that the methanogens in the different ponds are using different methanogenic pathways due to differences in salinities.

As previously mentioned, the most common methanogenic pathways in typical marine or freshwater settings are reduction of carbon dioxide using hydrogen gas or fermentation of acetate (Conrad, 2005). This is not true, however, in hypersaline environments where non-competitive substrates tend to dominate due to salinity constraints as well as because of the presence of sulfate. Carbon dioxide reduction has not been shown to occur at salinities greater than 88 ppt in culture studies and it has been suggested that it does not occur in the environment at salinities of more than 120 ppt (Oren, 1999). Acetoclastic methanogenesis does not occur at salinities higher than 60 ppt (Table 1; Oren, 1999).

Each of the different methanogenic substrates has a different range of fractionation factors associated with it (Table 1). In typical marine or freshwater settings, higher apparent fractionation factors are associated with CO_2 reduction, while lower apparent fractionation is associated with acetoclastic methanogenesis (Conrad, 2005). Interpreting the data in this way, Pond 1 and the natural marsh have apparent fractionation factors are similar to fractionation factors associated with methanogenesis from a combination of CO_2 reduction and acetoclastic methanogenesis, in Pond 4 the apparent fractionation factors are similar to fractionation factors linked to methanogenesis from CO_2 reduction, and in Pond 6 the apparent fractionation is close to the fractionation observed in acetoclastic methanogenesis. However, in this hypersaline system these interpretations do not make sense. The upper salinity tolerance of the acetoclastic methanogens is only 60 ppt (Table 1), and Pond 6 has a salinity of 106 ppt (Table 2), so the use of acetate as a methanogenic substrate is very unlikely in this setting. Therefore, the observed changes in apparent fractionation in the different ponds

can best be explained by changes in the relative importance of the different noncompetitive substrates.

The use of noncompetitive substrates in these ponds requires such substrates to be present. Dimethyl sulfide (DMS) has been detected in Ponds 4 and 5, and is thought to be the result of reactions between low molecular weight hydrocarbons and biogenic H_2S (Visscher et al., 2003). A small amount of methanogenesis from DMS has been shown to occur in these ponds as well (Visscher et al., 2003), therefore the isotopic signature of the methane may be at least partly due to this methanogenic pathway. Trimethylamine (TMA) is a breakdown product of glycine betaine, which is an osmoregulant used by halophilic cyanobacteria, anoxygenic photosynthetic bacteria, and halophilic methanogenic archaea (King, 1988; Summons et al., 1998; Oren, 2001). Although there are no previous reports of methylated amines in the hypersaline ponds of Guerrero Negro, it is likely to be present in significant quantities, and therefore is another candidate substrate for the methanogens in these environments. Methanol may be present as a degradation product of pectin (Conrad, 2005), though it has not been previously reported in these sites.

The nature of the substrates requires a rethinking of the manner of assessing apparent fractionation factors. For closer approximation of the apparent fractionation, it is necessary to use another possible carbon pool as a proxy for the methanogenic substrate. DMS, TMA, methanol or their precursors should be part of the mat material because they are degradation products of cellular materials and other organic substances in the mat. Therefore, it may be more reasonable to use the POM as a proxy for substrate than DIC. Figure 15 is a plot of the isotopic value of the methane against the $\delta^{13}C$ values

of the POM. Comparing these apparent fractionation factors (Table 3) with the known fractionation factors as well as the salinity tolerances of the organisms that use the various substrates leads to some conclusions about which substrates the methanogens are using in the different ponds.

Based on the salinity tolerances and fractionation factors associated with different methanogenic substrates, the methanogens in the low salinity sample sites (Pond 1 and the marsh) are either using CO_2 and H_2 or a combination of CO_2 and H_2 along with TMA as substrates. It is true that in typical marine settings methanogenesis from carbon dioxide is suppressed in the presence of sulfate due to competition for free hydrogen (King, 1983). The limitation of this resource leads to competition between microorganisms that require it as a substrate, particularly sulfate reducing bacteria and methanogens. In the salterns of the Exportadora de Sal de C. V., it has been shown that hydrogen is present in quantities that may be high enough to allow the methanogens to coexist with sulfate reducing bacteria (Hoehler et al., 2002). It has also been shown in previous experiments that lowering sulfate in the mats from Guerrero Negro stimulates methane production from carbon dioxide (Bebout et al., 2004). This indicates that the carbon dioxide reducing methanogens are present in the mat, albeit in small numbers (Smith et al., 2007). Therefore, it is possible that the apparent fractionation in Pond 1 may be at least partially due to reduction of carbon dioxide. Additionally, calculation of the fractionation factor for carbon dioxide at the temperatures of the Exportadora de Sal de C. V. salterns (between 16 and 20 °C, Table 2), using Equation 8 gives a range of fractionation factors between 1.058 and 1.059, which is similar to the observed apparent fractionation factor. Thus methanogenesis from reduction of carbon dioxide is possible

in the low salinity sites.

In Pond 4, the intermediate salinity pond, the predominant substrate is likely TMA, and possibly methanol as well. The apparent fractionation factors in this pond are in the range of fractionation factors associated with TMA, but they are slightly higher than in the low salinity sites. Some methanogenesis from methanol, which has a higher fractionation factor than TMA, would increase the apparent fractionation factor observed in this pond.

In Pond 6, the methanogens are most likely using DMS more than in the other ponds. The apparent fractionation factor in this pond is similar to that associated with acetoclasic methanogenesis, but the salinity tolerance of acetoclastic methanogens is 60 ppt. This is much less than the salinity observed at the site at the time of sampling, and the long range salinities (Table 2). The apparent fractionation factor in this pond is slightly lower than published fractionation factors associated with DMS (Table 1). The previously reported fractionation factors from DMS are reported from culture studies, and it may be that in the environment DMS has a wider range of fractionation factors than in these studies. The apparent fractionation factor observed in Pond 6 is more similar to fractionation factors from DMS than to those associated with other potential noncompetitive substrates. Thus, DMS is the most likely the substrate being used by methanogens in Pond 6.

The change from TMA in the lower salinity sites to DMS in the highest salinity site is interesting. It is possible that this change is due to a change in nitrogen cycling in the ponds. TMA contains nitrogen, and if nitrogen is limiting in higher salinities, it may be less available for methanogens. All the ponds are nitrogen limited (Des Marais,

1995), but possibly the higher salinity ponds are more limited by nitrogen since the water has been in the system for a longer period of time. It may also be that there is a change in the methanogenic community due to the increased salinity. Not all groups of methylotrophs are able to use DMS as a substrate; possibly the change in salinity makes this a more favorable substrate than TMA or methanol.

6. CONCLUSION

Samples of mat material and pore water from hypersaline microbial mats were taken along the salinity gradient contained within the salt works of the Exportadora de Sal de C. V., Baja California Sur, Mexico. Samples were also taken from mats maintained at the NASA Ames greenhouse facility. Measurements of the stable carbon isotopic composition of the POM, DIC and methane were made from these samples, measurements were also taken of the stable nitrogen isotopic composition, %C, and %N. The measurements of the $\delta^{13}C$ values of methane are the first reported from the pore water within these mats, and these values range from -49.6‰ to -74.1‰. The least negative $\delta^{13}C$ values were measured in the highest salinity site, and the most negative values were measured at the moderate salinity site.

The microbial mats located in these sites produce methane, despite the presence of abundant sulfate. In most marine and freshwater sediments, methanogenesis is suppressed in the presence of sulfate because the methanogens are outcompeted by sulfate reducing bacteria for key substrates, particularly hydrogen and acetate. Because methane is being produced in these ponds, it indicates that the methanogens are using noncompetitive substrates.

The apparent fractionation factors observed in the field sites change along a salinity gradient. These apparent fractionation factors are used in combination with known salinity tolerances of different methanogenic archaea to determine which methanogenic substrates are likely being used in the different ponds. Low salinity sites

(Pond 1 and the natural marsh) appear to be producing methane from CO_2 reduction or a combination of CO_2 reduction and trimethylamine (TMA). The moderate salinity pond (Pond 4) seems to be using primarily TMA. The highest salinity pond (Pond 6) appears to be using dimethylsulfide (DMS) as the primary substrate. Salinity may affect methanogenic substrate by changing the methanogenic communities present at different sites. Changing salinity may also be linked to other geochemical parameters (i. e. nitrogen availability) in this system that changes the methanogenic substrates available.

The microbial communities that are found in these hypersaline sites are considered to be unlithified counterparts of stromatolites, which were widespread on the early Earth. Methane produced by microbial activity may have been important on the early Earth. Measurements of the stable carbon isotopes of methane produced at these hypersaline sites may be applicable to study of early life on Earth. Methane is also an important candidate biosignature gas. Characterization of the stable carbon isotopic composition of methane produced in hypersaline environments may aid in the search for life on other planets.

7. REFERENCES

Bebout, B. M., Carpenter, S. P., Des Marais, D. J., Discipulo, M., Embaye, T., Garcia-Pichel, F., Prufert-Bebout, L. E., Raleigh, C., Rothrock, M., Turk, K., Long-term manipulations of intact microbial mat communities in a greenhouse collaboratory: Simulating Earth's present and past field environments, Astrobiology, v. 2, p. 383-402, 2002.

Bebout, B. M., Hoehler, T. M., Thamdrup, B., Albert, D., Carpenter, S. P., Hogan, M., Turk, K., Des Marais, D. J., Methane production by microbial mats under low sulphate conditions, Geobiology, v. 2, p 87-96, 2004.

Brenna, J.T, Corso, T.N, Tobias, H.J, Caimi, R.J, High-precision continuous-flow isotope ratio mass spectrometry, Mass Spectrometry Reviews, v. 16, p. 227-258, 1997.

Conrad, R., Quantification of methanogenic pathways using stable carbon isotopic signatures: a review and a proposal, Organic Geochemistry, v. 36, p. 739-752, 2005.

Canfield, D. E., Des Marais, D. J., Aerobic sulfate reduction in microbial mats, Science, v. 251, p. 1471-1473, 1991.

Canfield, D. E., Des Marais, D. J., Biogeochemical cycles of carbon, sulfur, and free oxygen in a microbial mat, Geochemica et Cosmochimica Acta, v. 57, p. 3971-3984, 1993.

Craig, H., Isotopic standards for carbon and oxygen and correction factors for mass spectrometric analysis of carbon dioxide, Geochimica et Cosmochimica Acta, v. 12, p. 133-149, 1957.

Davis, J. C., Statistics and data analysis in geology, 2nd Edition, John Wiley & Sons, New York, 1986.

Des Marais, D. J., Biogeochemistry of hypersaline microbial mats illustrates the dynamics of modern microbial ecosystems and the early evolution of the biosphere, Biological Bulletin, v. 204, p. 160-167, 2003.

Des Marais, D. J. and Canfield, D. E., The carbon isotope biogeochemistry of microbial mats, Microbial mats: Structure, development and environmental significance, edited by L. Stal and P. Caumette, Springer-Verlag, Berlin, p. 289-298, 1994.

Des Marais, D.J., Cohen, Y., Nguyen, H., Cheatham, M., Cheatham T., Munoz, E., Carbon isotopic trends in the hypersaline ponds and microbial mats at Guerrero Negro, Baja California Sur, Mexico: Implications for Precambrian stromatolites, Microbial Mats: Physiological Ecology of Benthic Microbial Communities, edited by Y. Cohen and E. Rosenberg, American Society for Microbiology, Washington D.C., p. 191-203, 1989.

Faure, G., Principles of Isotope Geology, 2nd Edition, John Wiley & Sons, New York, 1986.

Fogel, M. L., and Cifuentes , L. A., Isotope fractionation during primary production, Organic geochemistry, edited by M. Engel and S. Macko, Plenum Press, New York, p. 73-98, 1993.

Garcia, J. L., Patel, B. K. C., Ollivier, B., Taxonomic, phylogenetic, and ecological diversity of methanogenic Archaea, Anaerobe, v. 6, p. 205-226, 2000.

Garcia-Pichel, F., Mechling, M., Castenholz, R. W., Diel migrations of microorganisms within a benthic, hypersaline mat community, Applied and Environmental Microbiology, v. 60, p. 1500-1511, 1994.

Garrett, P., Phanerozoic stromatolites: noncompetitive ecologic restriction by grazing and burrowing animals, Science, v. 169, p. 171-173, 1970.

Hedges, J.I., Stern, J.H, Carbon and nitrogen determinations of carbonate-containing solids, Limnology and Oceanography, v. 29, p. 657-663, 1983.

Hoefs, J., Stable Isotope Geochemistry, 5th edition, Springer-Verlag, Berlin, 2004.

Hoehler, T.M., Bebout, B.M, Des Marais, D.J., The role of microbial mats in the production of reduced gases on the early Earth, Nature, v. 412, p. 324-327, 2001.

Hoehler, T. M., Albert, D. B., Alperin, M. J., Bebout, B. M., Martens, C. S., Des Marais, D. J., Comparative ecology of H_2 cycling in sedimentary and phototrophic ecosystems, Antonie van Leeuwenhoek, v. 81, p. 575-585, 2002.

Junk, G., Svec, H., The absolute abundance of the nitrogen isotopes in the atmosphere and compressed gas from various sources, Geochimica et Cosmochimica Acta, v. 14, p. 234-243, 1958.

Kasting, J. F., Methane and climate during the Precambrian era, Precambrian Research, v. 137, p. 119-129, 2005.

Kelley, C.A., Prufert-Bebout, L.E., Bebout, B.M., Changes in carbon cycling ascertained by stable isotopic analyses in a hypersaline microbial mat, Journal of Geophysical Research, v. 111, G04012, doi: 10.1029/2005JG000212, 2006.

King, G. M., Methanogenesis from methylated amines in a hypersaline algal mat, Applied and Environmental Microbiology, v. 54, p. 130-136, 1988.

King, G. M., Klug, M. J., Lovley, D. R., Metabolism of acetate, methanol, and amines in intertidal sediments of Lowes Cove, Maine, Applied and Environmental Microbiology, v. 45, p. 1848-1853, 1983.

Ley, R.E., Harris, J.K., Wilcox, J., Spear, J.R., Miller, S.R., Bebout, B.M., Maresca, J.A., Bryant, D.A., Sogin, M.L., Pace, N.R., Unexpected diversity and complexity of the Guerrero Negro hypersaline microbial mat, Applied and Environmental Microbiology, v. 72, p. 3685-3695, 2006.

Minawaga, M. and Wada E., Stepwise enrichment of ^{15}N along food chains: Further evidence and the relation between $\delta^{15}N$ and animal age, Geochimica et Cosmochimica Acta, v. 48, p. 1135-1140, 1984.

Oren, A., Formation and breakdown of glycine betaine and trimethylamine in hypersaline environments, Antonie van Leeuwenhoek, v. 58, p. 291-298, 1990.

Oren, A., Bioenergetic aspects of halophilism, Microbiology and Molecular Biology Reviews, v. 63, p. 334-348, 1999.

Oren, A., The bioenergetic basis for the decrease in metabolilc diversity at increasing salt concentration: implications for the functioning of salt lake ecosystems, Hydrobiologia, v. 466, p. 61-72, 2001.

Oren A., Diversity of halophilic microorganisms: Environments, phylogeny, physiology, and applications, Journal of Industrial Microbiology & Biotechnology, v. 28, p. 56-63, 2002.

Pavlov, A. A., Hurtgen, M. T., Kasting, J. F., Arthur, M. A., Methane-rich Proterozoic atmosphere?, Geology, v. 31, p. 87-90, 2003.

Redfield, A. C., Ketchum, B. J., Richards, F. A., The influence of organisms on the composition of sea water, The Sea, v. 2, p. 26-77, edited by M. Hill, Wiley Interscience, New York, 1963.

Rice, A.L., Gotoh, A.A., Ajie, H.O., Tyler, S.C., High-P\precision continuous-flow measurement of $\delta^{13}C$ and δD of atmospheric CH_4, Analytical Chemistry, v. 73, p. 4104-4110, 2001.

Shumilin, E., Grajeda-Muñoz, M., Silverberg, N., Sapozhnikov, D., Observations on trace element hypersaline geochemistry in surficial deposits of evaporation ponds of Exportadora de Sal, Guerrero Negro, Baja California Sur, Mexico, Marine Chemistry, v. 79, p. 133-153, 2002.

Smith, J. M., Green, S. J., Kelley, C. A., Prufert-Bebout, L., Bebout, B. M., Shifts in methanogenic community structure and function associated with long-term manipulation of sulfate and salinity in a hypersaline microbial mat, Environmental Microbiology, in review, 2007.

Summons, R. E., Franzmann, P. D., Nichols, P. D., Carbon isotopic fractionation associated with methylotrophic methanogenesis, Organic Geochemistry, v. 28, p. 465-475, 1998.

Van Leerdam, R. C., de Bok, F. A. M., Lomans, B. P., Stams, A. J. M., Lens, P. N. L., Janssen, A. J. H., Volatile organic sulfur compounds in anaerobic sludge and sediments: biodegradation and toxicity, Environmental Toxicology and Chemistry, v. 25, p 3101-3109, 2006.

Visscher, P. T., Baumbartner, L. K., Buckley, D. H., Rogers, D. R., Hogan, M. E., Raleigh, C. D., Turk, K. A., Des Marais, D. J., Dimethyl sulphide and methanethiol formation in microbial mats: potential pathways for biogenic signatures, Environmental Microbiology, v. 5, p. 296-308, 2003.

Walter, M. R., Archean stromatolites: Evidence of the Earth's earliest benthos, Earth's Earliest Biosphere, edited by J. W. Schopf, Princeton Univ. Press, Princeton, NJ, p. 187-213, 1983.

Whiticar, M. J., Carbon and hydrogen isotope systematics of bacterial formation and oxidation of methane, Chemical Geology, v. 161, p. 291-314, 1999.

Whitley, E., Ball, J., Statistics review 3: Hypothesis testing and P values, Critical Care, v. 3, p. 222-225, 2002.

8. FIGURES

Figure 1. Map of the area surrounding Guerrero Negro, after Shumilin et al., 2002, including the salterns of the Exportadora de Sal de C. V., Baja California Sur, Mexico. Inset shows the location of Guerrero Negro in Baja California. Concentration ponds are shown in white, with locations of study sites indicated by letters: (a) Pond 6, (b) natural marsh, (c) Pond 4, and (d) Pond 1.

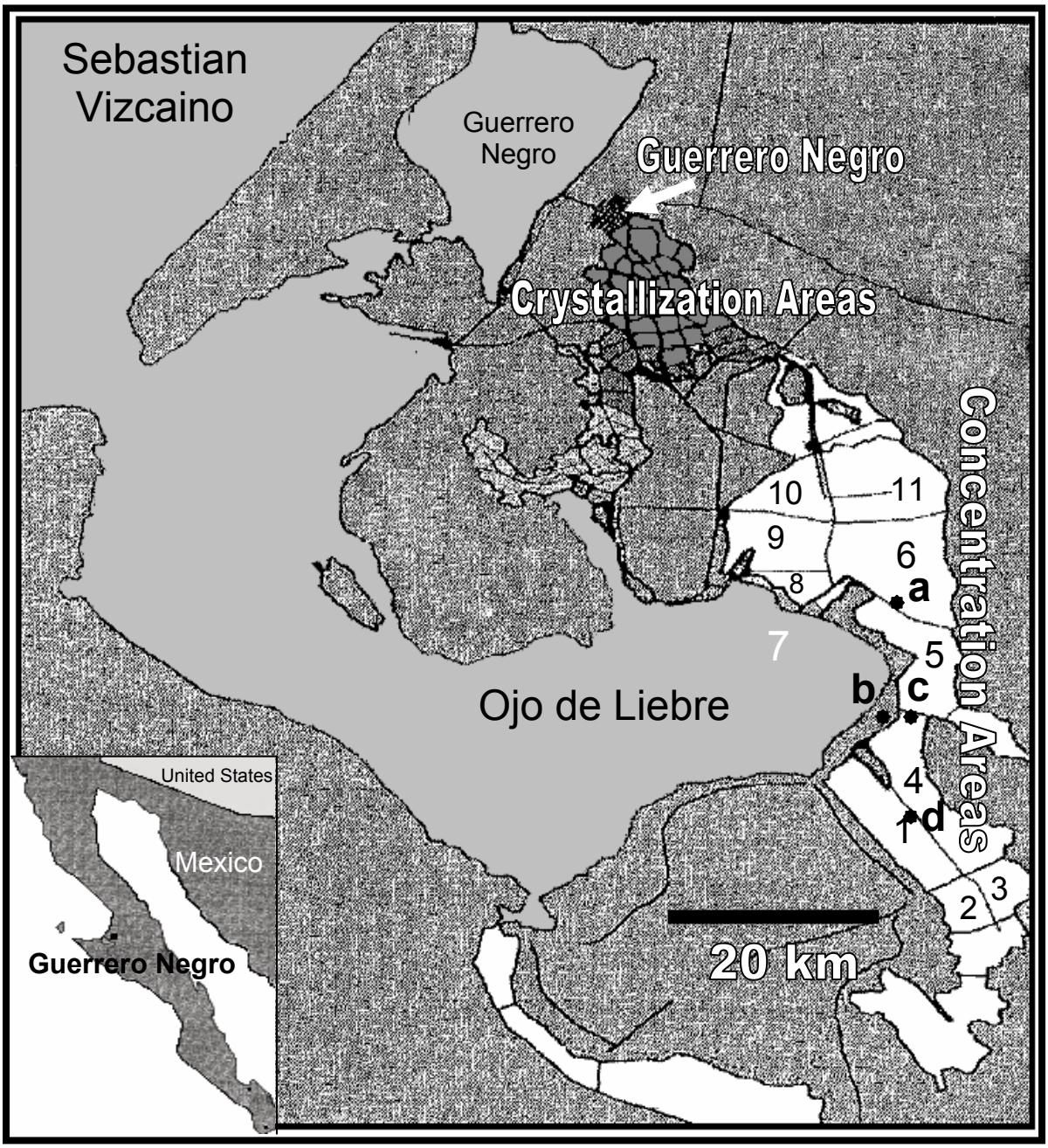

Figure 2. Depth profiles of methane production (nmol/hr/g) in the mats sampled in situ (B. M. Bebout, unpublished data). These data were measured from three time points.

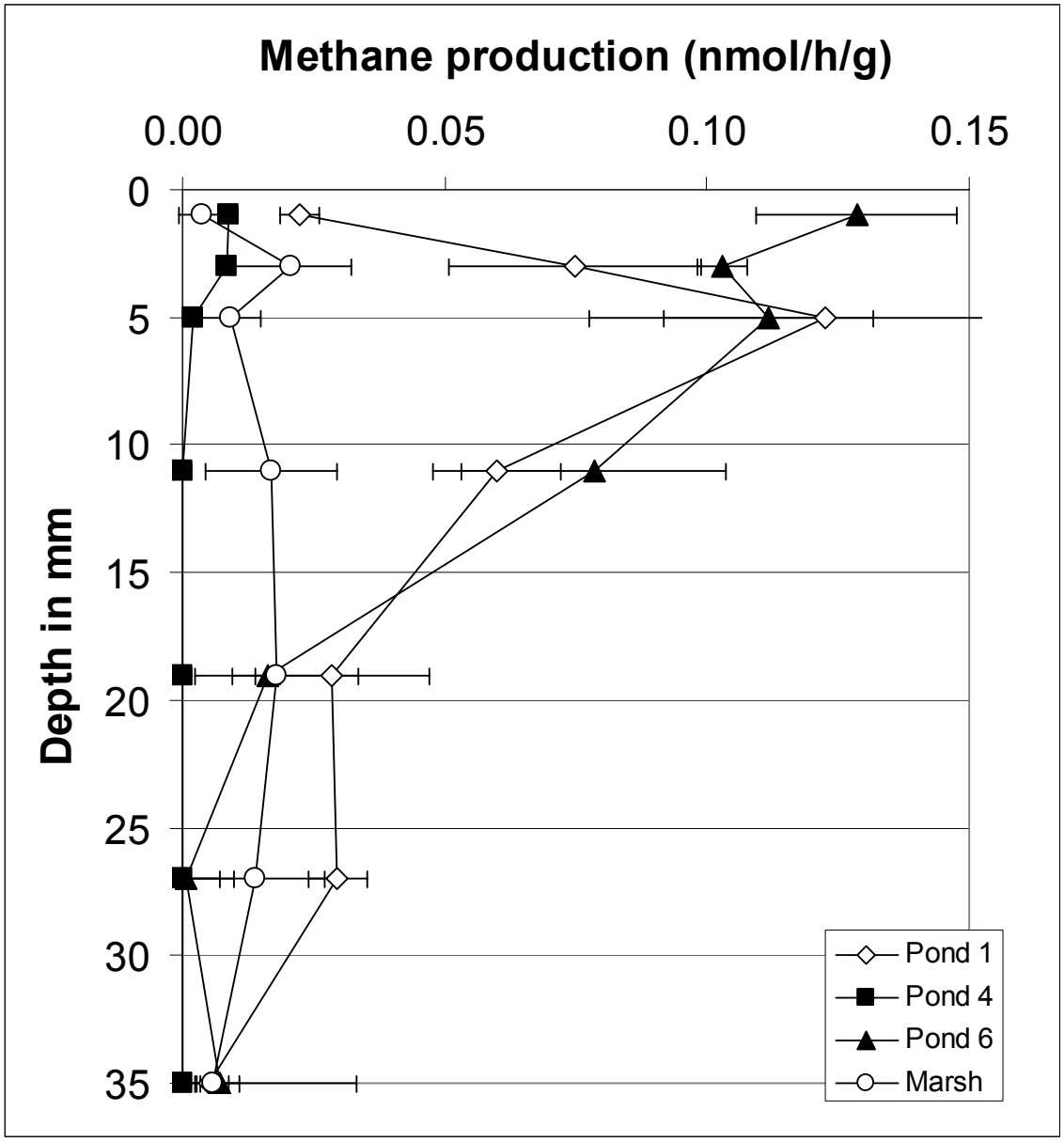

Figure 3. Depth profiles of methane concentration (μM) in the field sites (B. M. Bebout, unpublished data). The negative depth values indicate measurements of methane taken from the water overlying the mats.

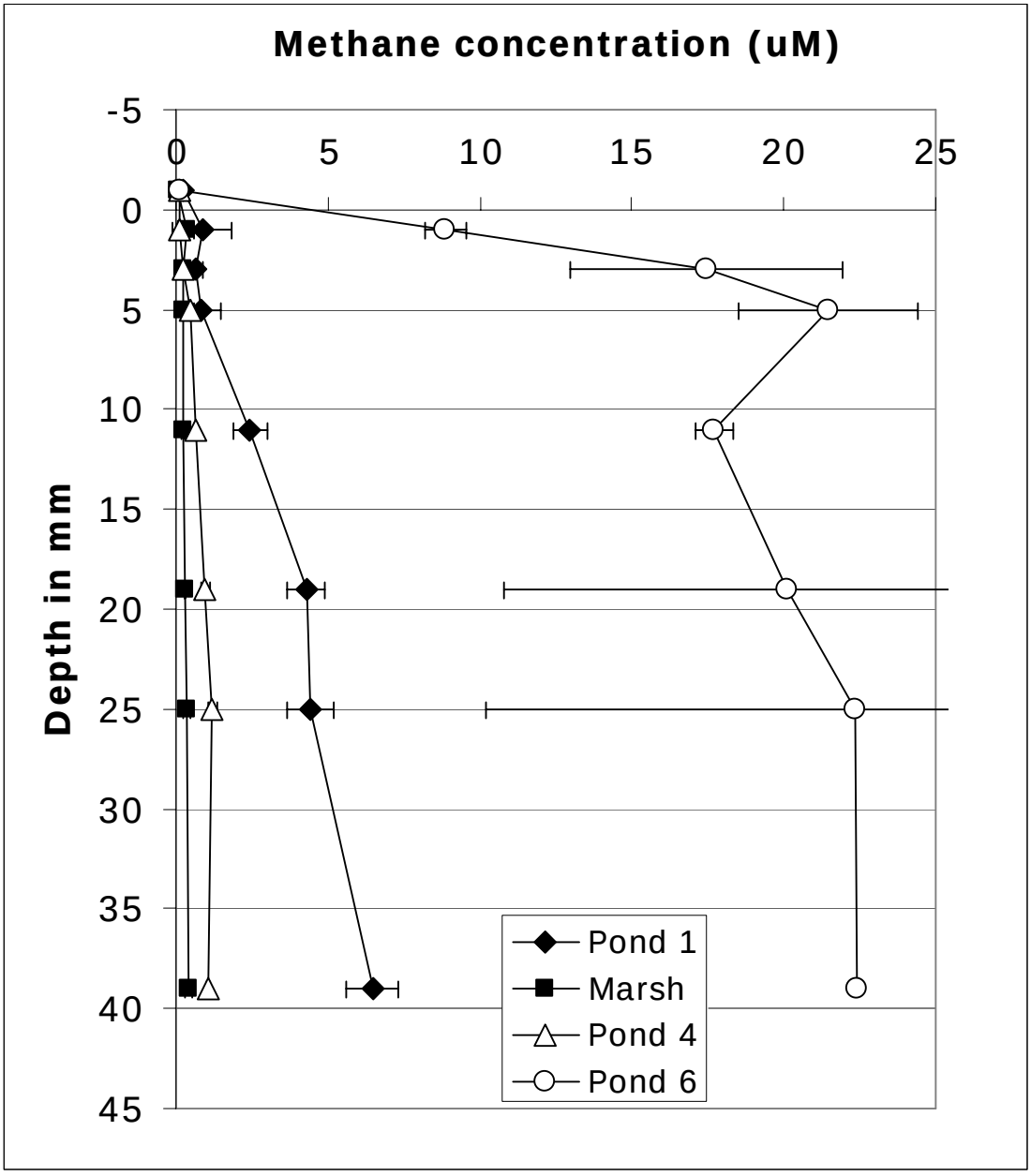

Figure 4. Depth profiles of $\delta^{13}C$ values of dissolved inorganic carbon (DIC) from mats maintained at the NASA Ames greenhouse facility and mats growing in Pond 4. Error bars represent one standard deviation about the mean of triplicate samples.

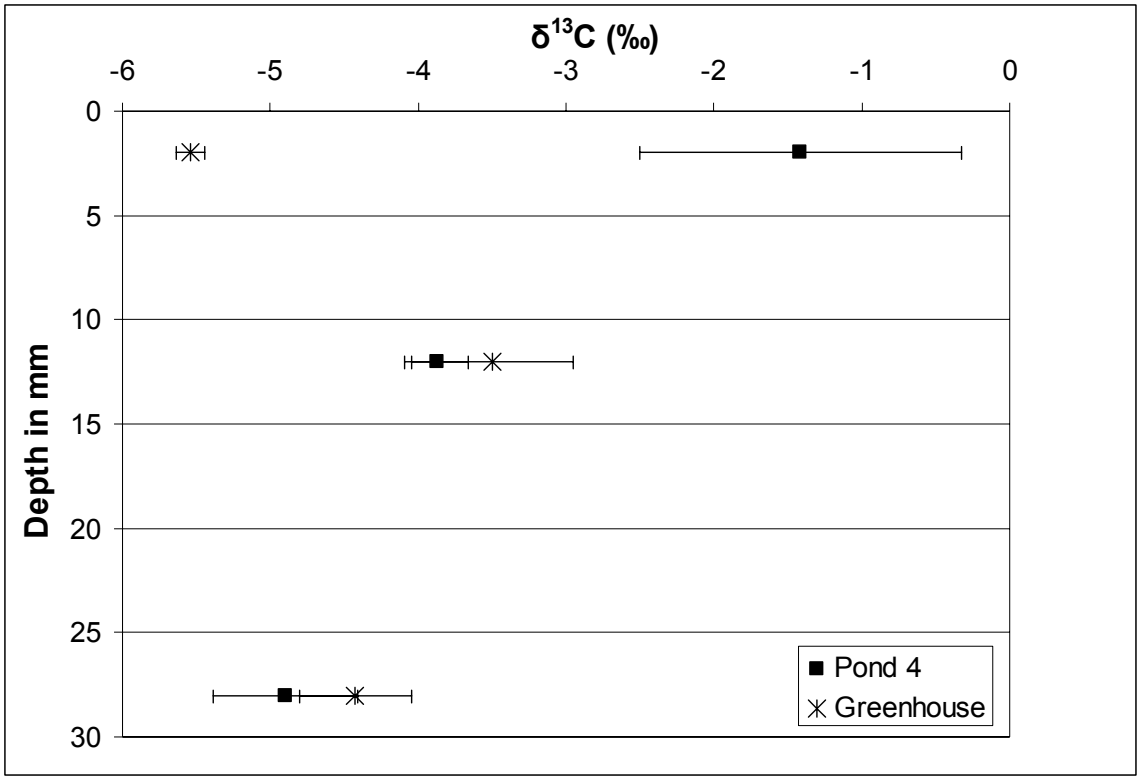

Figure 5. Depth profiles of $\delta^{13}C$ values of the dissolved inorganic carbon (DIC) within the in situ mats. Error bars represent one standard deviation.

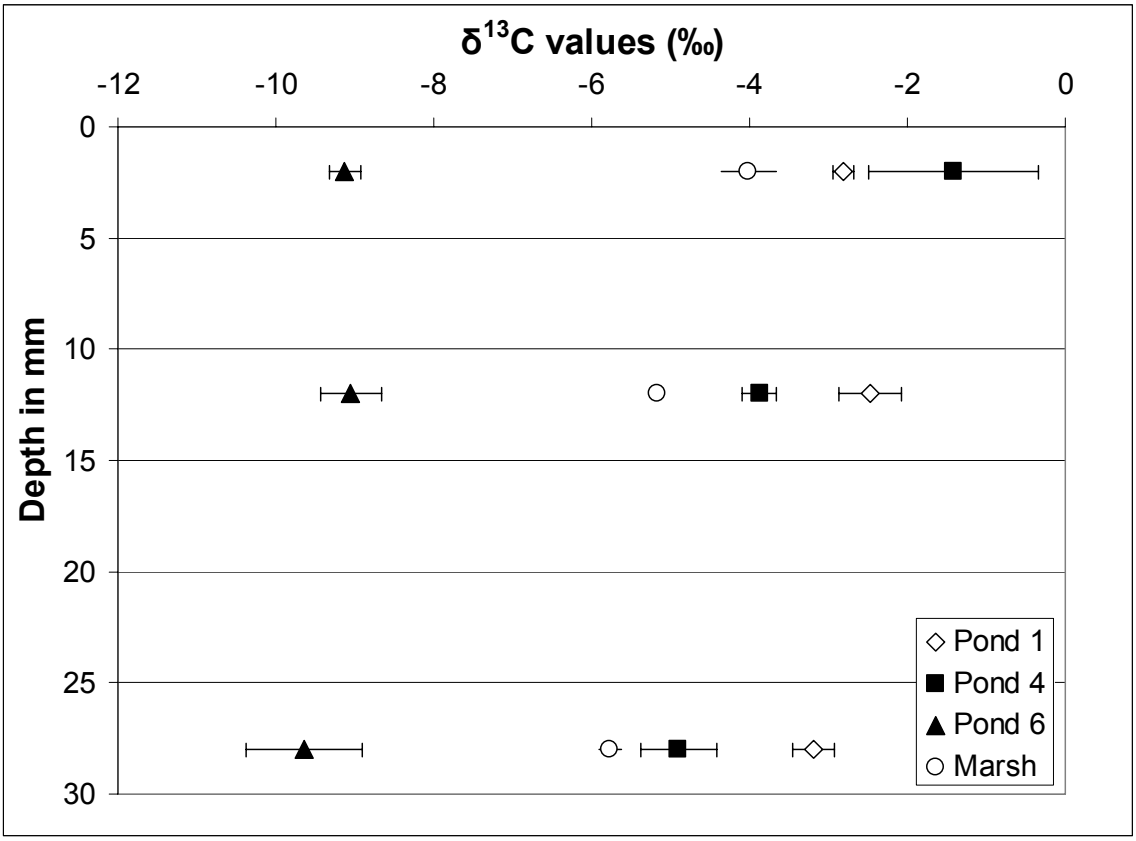

Figure 6. Depth profile of dissolved inorganic carbon (DIC) concentration (mM) in the in situ mats. The error bars represent one standard deviation about the mean.

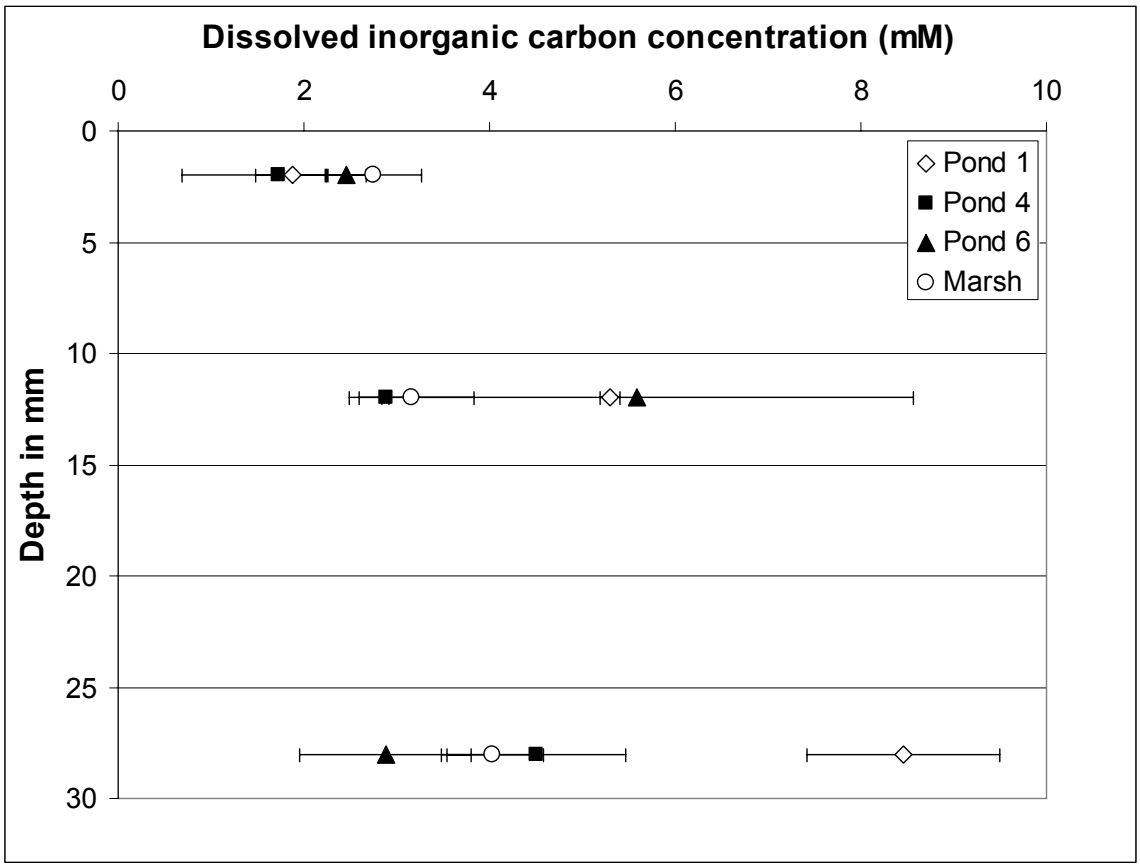

Figure 7. Depth profile of dissolved inorganic carbon (DIC) concentration (mM) of Pond 4 mats and mats maintained in the greenhouse facility. The error bars represent one standard deviation about the mean.

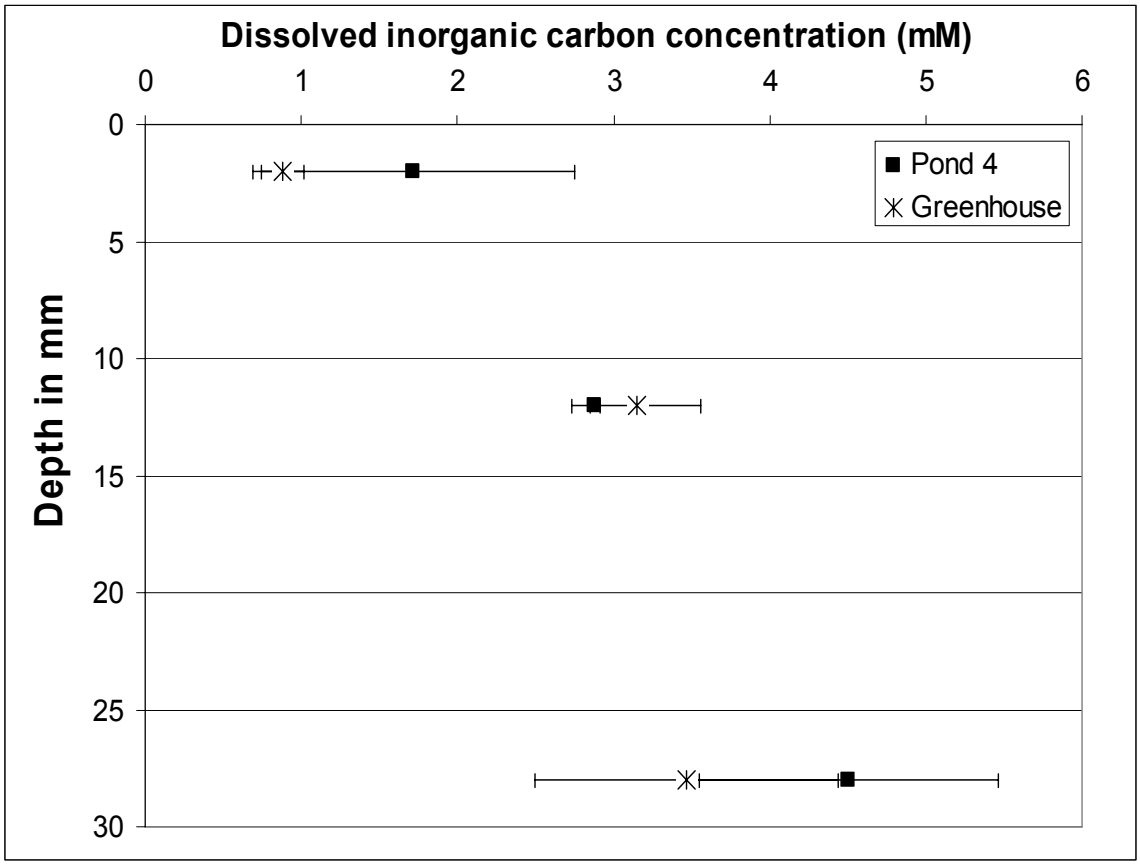

Figure 8. Depth profiles of $\delta^{13}C$ values of the particulate organic matter (POM) within the mats sampled in situ. Error bars represent one standard deviation.

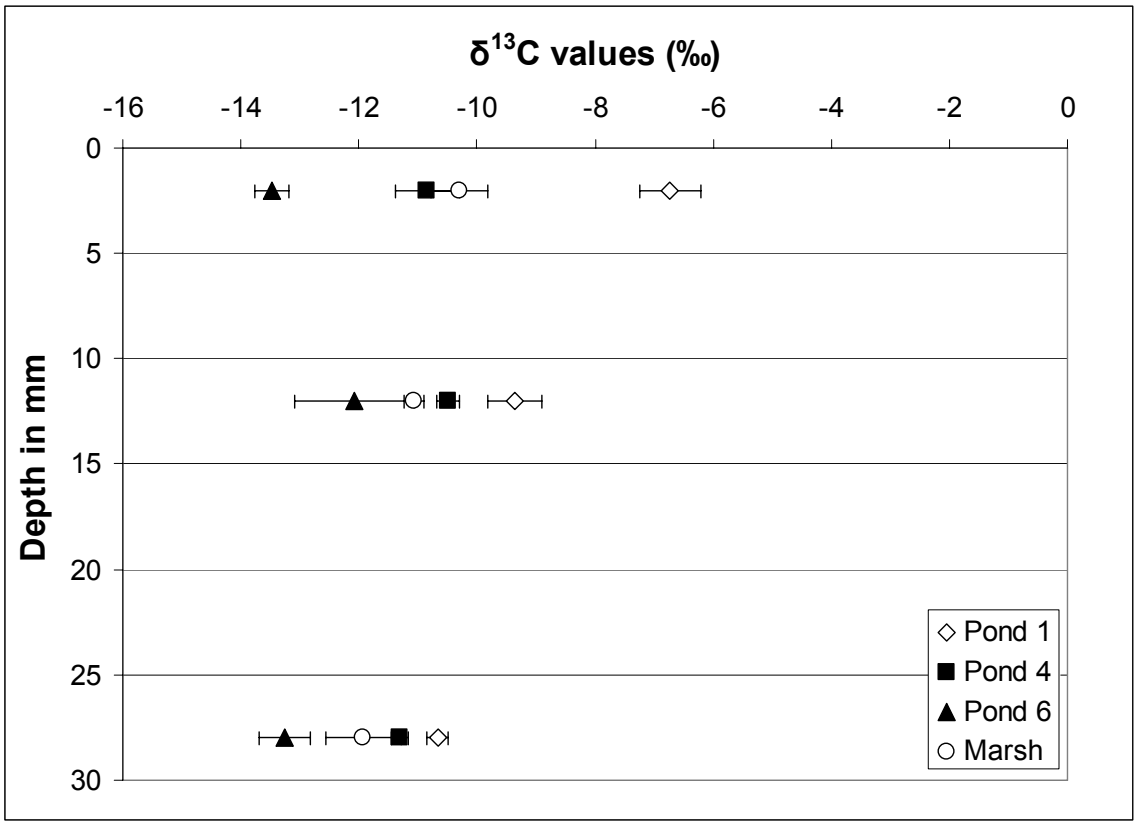

Figure 9. Depth profiles of $\delta^{15}N$ values of the particulate organic matter (POM) within the mat. Error bars represent one standard deviation.

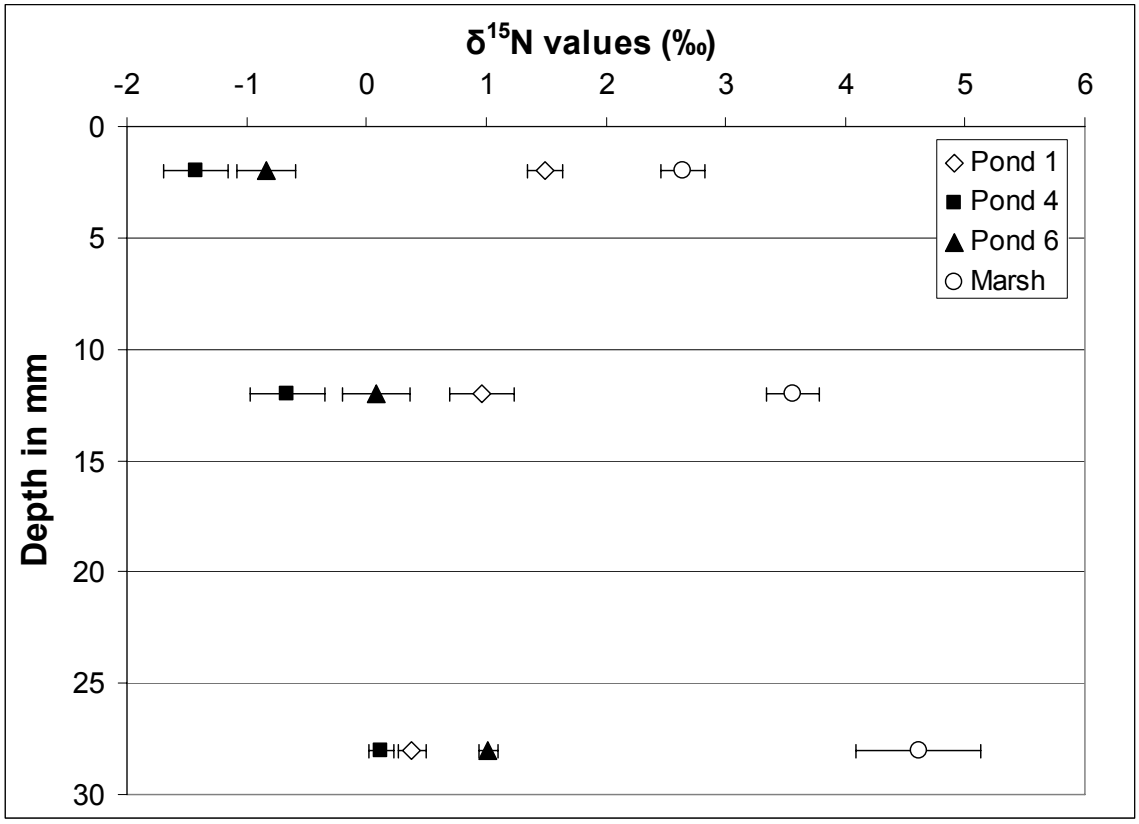

Figure 10. Depth profiles of the carbon to nitrogen ratio (C/N) in the mats sampled in situ. Error bars represent one standard deviation.

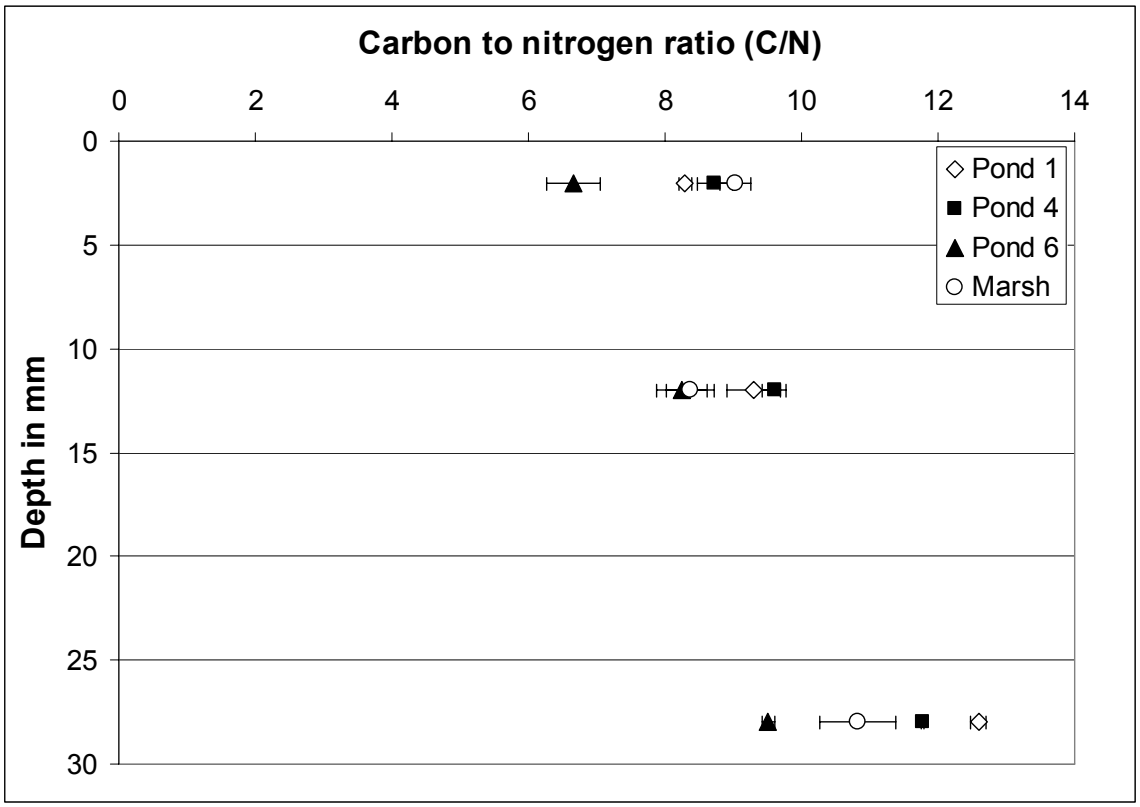

Figure 11. Depth profiles of $\delta^{13}C$ of methane in mats sampled in Pond 4 and from mats maintained in the greenhouse facility. The isotopic composition of the methane in the greenhouse mats was measured from both one and two slices of mat core.

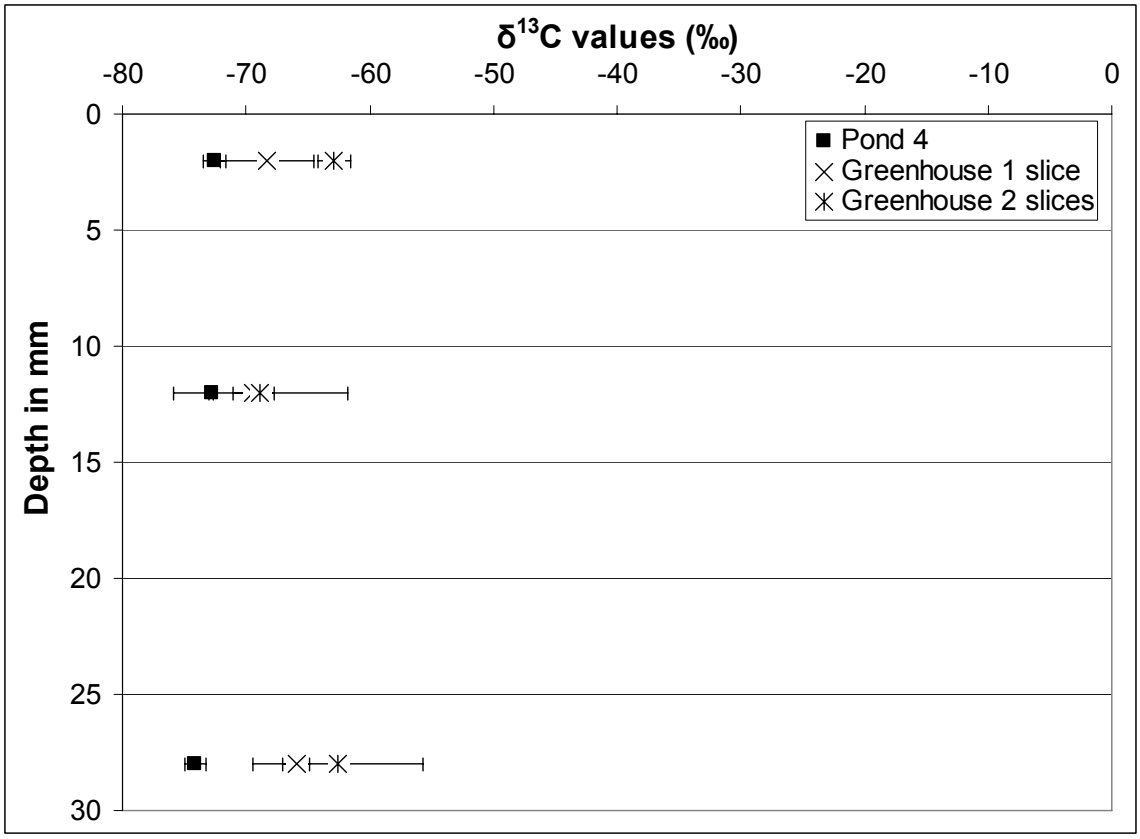

Figure 12. Depth profiles of $\delta^{13}C$ of methane from the in situ mats. Error bars represent one standard deviation.

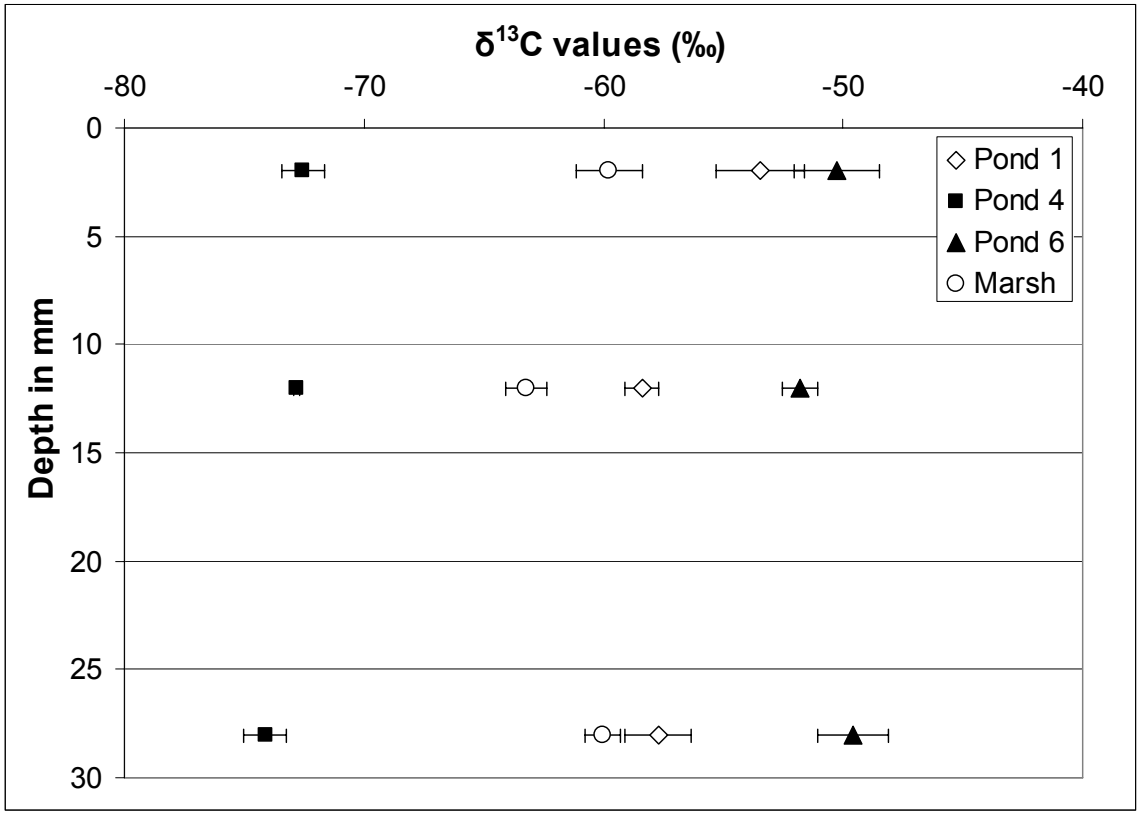

Figure 13. Difference between the $\delta^{13}C$ of dissolved inorganic carbon (DIC) and the $\delta^{13}C$ of particulate organic matter (POM). Error bars represent one standard deviation.

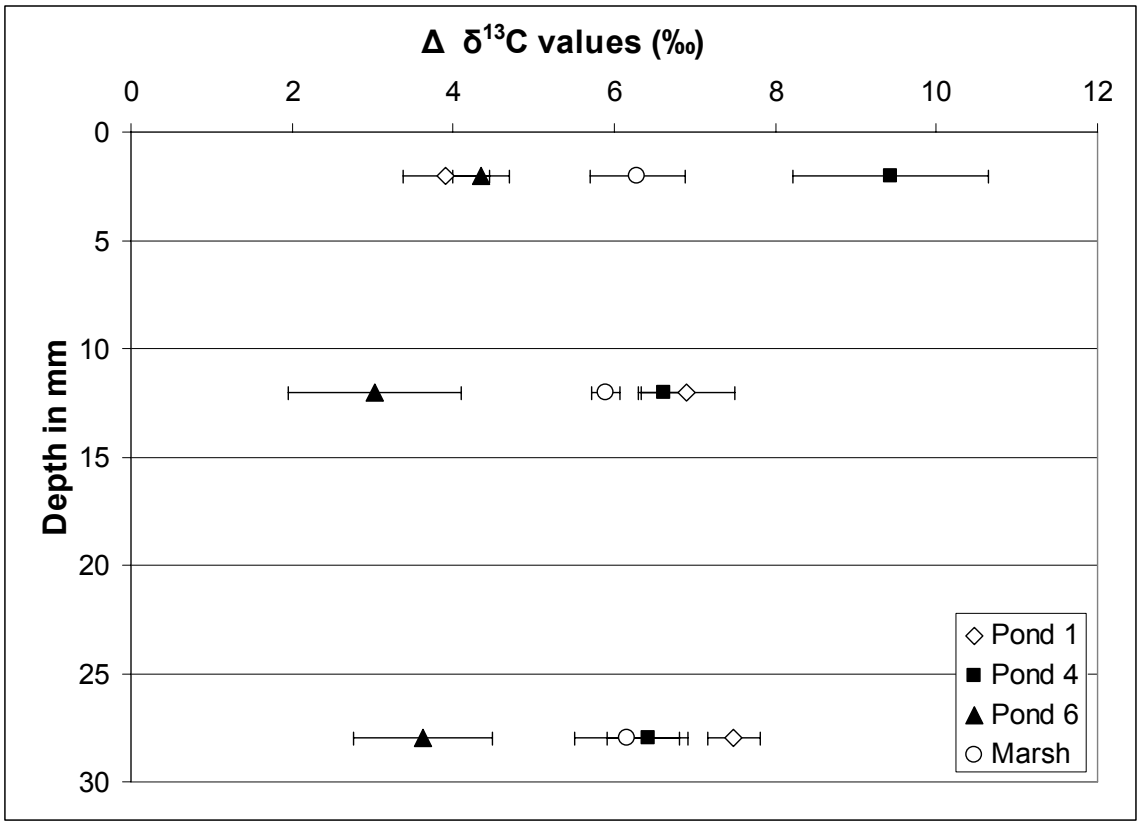

Figure 14. $\delta^{13}C$ values of methane plotted against the $\delta^{13}C$ values of dissolved inorganic carbon (DIC). The numbered lines indicate equal fractionation factors. Error bars represent one standard deviation.

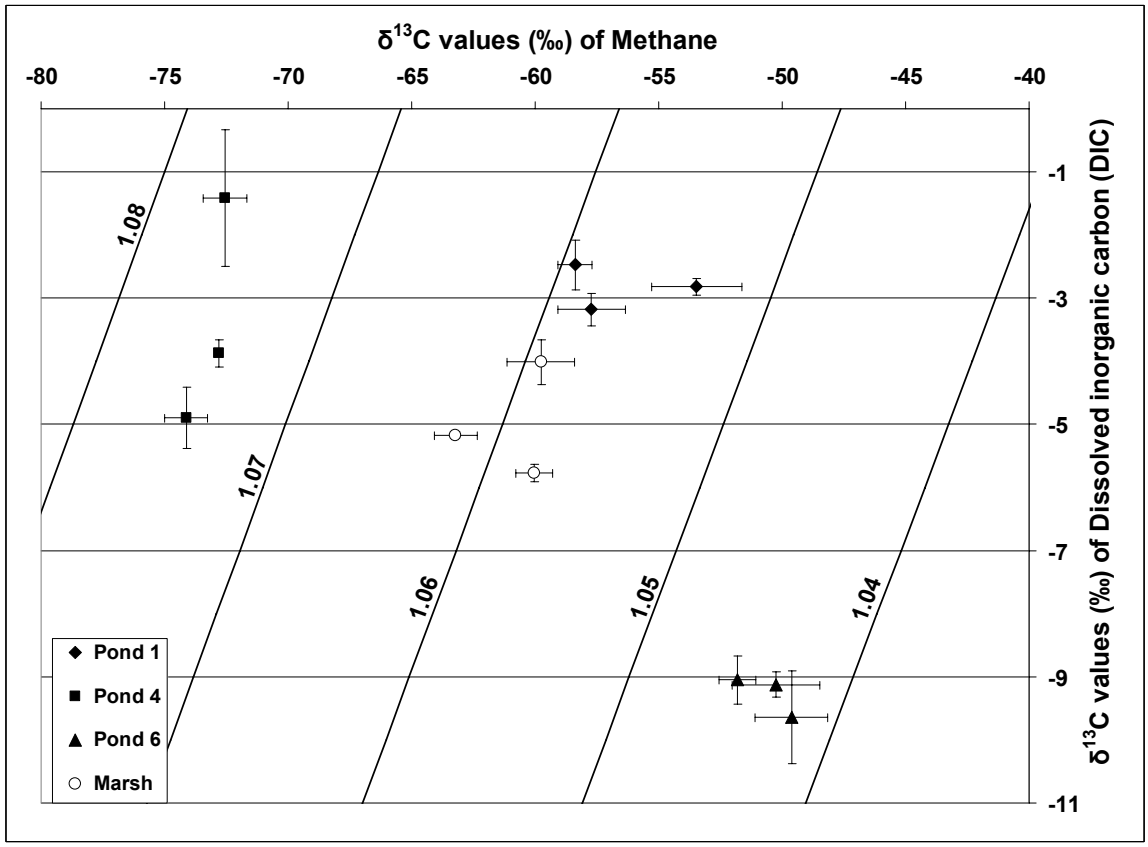

Figure 15. $\delta^{13}C$ of methane vs. $\delta^{13}C$ of particulate organic matter (POM). The numbered lines represent equal fractionation factors. Error bars represent one standard deviation.

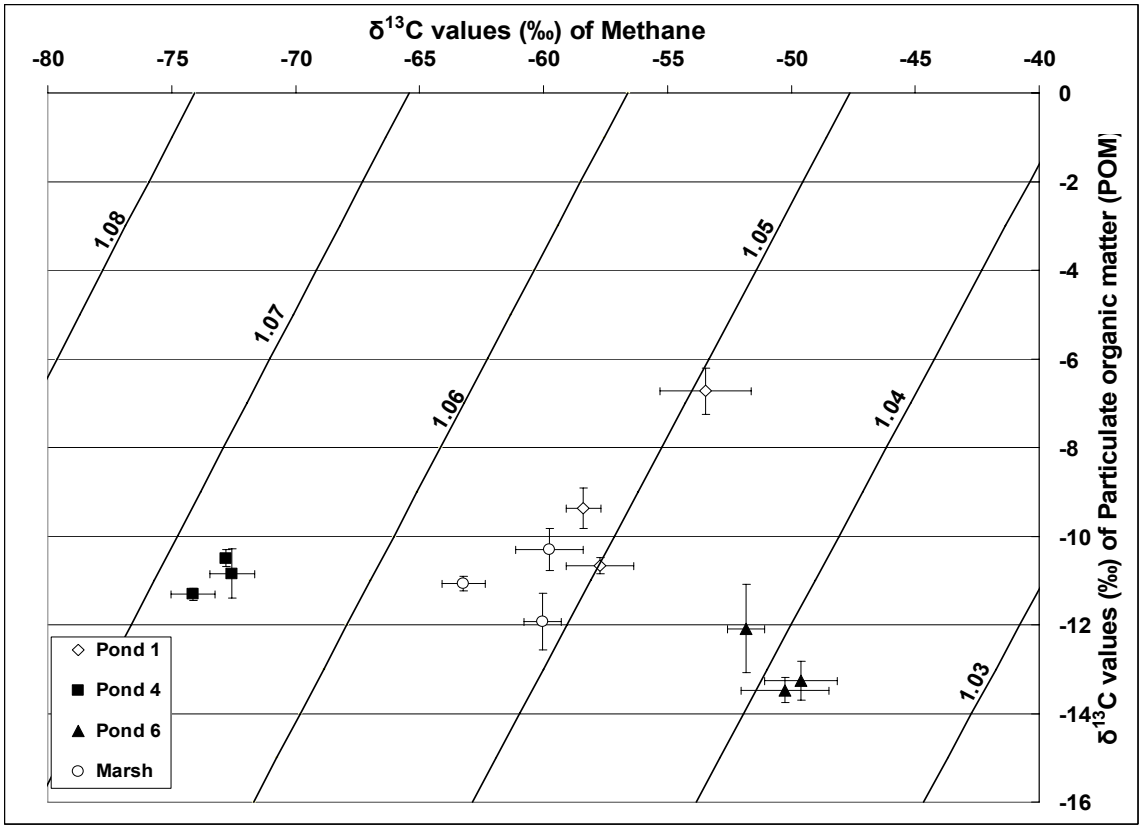

APPENDIX

1. DATA TABLES

Nitrogen data. Raw nitrogen data from the MU IRMS lab.

Sample	Weight (mg)	Amplitude	Background 28(mV)	Area (Vs)	δ15N vs AIR	%Nitrogen	calculated mg N	bulk sample %N
Pond 1 0-4A	14.405	7972	4.7	344.757	1.375	4.1365791	0.505012702	4.078441204
Pond 1 0-4A	16.188	8547	5.5	371.858	1.24	3.9925264	0.542864669	3.901247906
Pond 1 0-4A	6.144	2526	4.8	113.124	1.487	3.1538107	0.180159804	3.411236741
Pond 1 0-4B	16.635	10119	5.6	432.853	1.25	4.3609175	0.628056385	4.353460342
Pond 1 0-4B	5.986	2869	4.3	128.736	1.155	3.8861401	0.203515356	3.920299382
Pond 1 0-4C	14.024	9153	5.8	395.414	1.038	4.8628523	0.575765334	4.511059939
Pond 1 0-4C	5.512	3174	4.1	141.694	1.167	4.4449542	0.22900524	4.443312601
Pond 1 10-14A	22.178	4527	5.1	200.872	1.001	1.6858498	0.304048522	1.69868548
Pond 1 10-14B	20.113	2934	4.9	130.438	0.583	1.2768593	0.205673355	1.299582391
Pond 1 10-14C	23.896	2308	5.1	103.034	0.5	0.9223027	0.167398188	0.886661358
Pond 1 26-30A	19.91	2424	5.9	108.697	-0.006	1.1930791	0.1753077	1.078029214
Pond 1 26-30A	17.506	2160	5.4	96.886	0.028	1.1912096	0.158811276	1.110696006
Pond 1 26-30B	22.351	2823	5.2	125.683	0.232	1.1549324	0.199032046	1.128998263
Pond 1 26-30C	22.063	2228	5.3	99.159	0.176	0.982768	0.161985975	0.909432684
Pond 4 0-4A	9.365	4657	4.8	209.894	-1.543	3.9323457	0.31664955	3.83779239
Pond 4 0-4B	20.079	6696	4.4	302.412	-1.946	2.6708901	0.463334652	2.567063319
Pond 4 0-4C	12.65	6606	5.0	290.41	-1.474	4.0299427	0.44537966	3.894090682
Pond 4 10-14A	15.45	3320	4.4	143.221	-0.486	1.702404	0.225184916	1.677145837
Pond 4 10-14B	15.431	4393	4.1	192.859	-1.255	2.2719285	0.299443364	2.12520407
Pond 4 10-14C	15.923	3398	5.2	151.903	-0.886	1.8613696	0.23565352	1.744854719
Pond 4 10-14C	15.184	3211	5.1	141.797	-0.974	1.8397355	0.22153847	1.720177223
Pond 4 26-30A	16.016	3654	4.6	163.61	0.033	0.0070943	0.012178452	1.782256108
Pond 4 26-30B	16.145	3883	4.4	170.959	-0.109	1.9935222	0.266680964	1.806434171
Pond 4 26-30C	15.625	3478	5.0	153.81	-0.172	1.9324755	0.24102606	4.558233768
Pond 6 0-4A	33.671	8581	5.0	367.776	-1.132	1.879037	0.537163339	1.792629837
Pond 6 0-4B	25.734	2918	4.9	131.768	-0.862	1.0053624	0.207530966	0.868562622
Pond 6 0-4C	28.42	4672	5.1	211.393	-1.348	1.3359646	0.318743203	1.2912953
Pond 6 10-14A	24.232	3325	4.8	150.724	-0.126	1.2151851	0.234006811	1.123379276
Pond 6 10-14B	15.673	3157	5.0	143.651	-0.496	1.7232498	0.224127952	0.984521839
Pond 6 10-14C	30.83	3900	4.7	174.796	0.058	1.0504845	0.267628173	1.03757561
Pond 6 26-30A	19.111	3466	4.9	153.554	0.681	1.5298416	0.237959472	1.39710804
Pond 6 26-30B	18.49	3491	5.7	156.069	0.833	1.700265	0.241472172	1.469263363
Pond 6 26-30C	18.112	3750	5.3	165.361	0.719	1.7903266	0.254450309	1.588780659
Marsh 0-4A	28.551	4998	4.8	212.716	2.265	1.3975397	0.329149436	1.455113683
Marsh 0-4B	20.554	3237	4.5	140.066	2.633	1.3106588	0.220465036	1.389189795
Marsh 0-4C	20.273	3423	4.7	152.104	2.341	1.4414398	0.235934257	1.494152862
Marsh 10-14A	40.735	2966	4.6	128.457	3.198	0.6733941	0.203097972	0.591708868
Marsh 10-14B	36.995	2881	4.5	127.634	3.266	0.7122096	0.201866764	0.674973891
Marsh 10-14C	28.775	1467	4.3	63.737	3.608	0.3909528	0.106276852	0.436075007
Marsh 26-30A	45.04	1333	4.3	57.483	4.654	0.2418351	0.069920868	0.260427972
Marsh 26-30B	41.689	1758	4.2	76.786	4.748	0.3710492	0.125798156	0.373265613
Marsh 26-30C	67.356	2031	4.3	91.776	3.809	0.2974446	0.148223196	0.254691593

DIC data. Raw DIC data from the MU IRMS lab.

Sample site	Depth	Approx sampl vol (uL)	approx sum CO2 (mM)	volume of acid (uL)	volume of He (vol. injected in G (umol CO2	approx mV	estimated mV	meas 44 amp Vs	meas area	δ13C	δ13C corrected	Calculated moles of CO2	Calculated [CO2]	depth
Pond 1	0-4 A	350	2	1000	690	0.0061536	1607.404	1964	49.217	-2.394	-2.9336667	9.52087E-05	2.21120013	2
Pond 1	10-14 A	500	6	1000	500	40 0.24	4477.768	5383	134.088	-1.805	-2.0536667	0.0002073	5.1846461	12
Pond 1	26-30 A	500	6	1000	500	40 0.24	4477.768	7662	191.497	-2.653	-2.9016667	0.0002961	7.4044232	28
Pond 1	0-4 B	380	2	1000	620	70 0.0058064	1600.922	1670	40.159	-2.595	-2.8436667	6.21115E-05	1.4477116	2
Pond 1	10-14 B	500	6	1000	500	20 0.12	2238.884	2855	69.693	-2.279	-2.5276667	0.0001077	5.3894988	12
Pond 1	26-30 B	500	6	1000	500	20 0.12	2238.884	4669	109.831	-2.961	-3.2236667	0.0001686	8.4034501	28
Pond 1	0-4 C	500	2	1000	500	80 0.16	2985.179	4305	101.881	-2.426	-2.6746667	0.0001575	1.9666521	2
Pond 1	10-14 C	500	6	1000	500	20 0.12	2238.884	2898	68.739	-2.592	-2.8406667	0.0001063	5.315723	12
Pond 1	26-30 C	500	6	1000	500	15 0.09	1679.163	3975	91.979	-3.169	-3.4176667	0.0001422	9.4838925	28
Pond 4	0-4 A	290	2	1000	710	80 0.0653211	1219.298	2027	47.424	1.119	0.7933333	9.17402E-05	2.807766	2
Pond 4	10-14 A	390	6	1000	610	50 0.1918033	3578.544	1832	47.606	-3.515	-4.054667	9.32922E-05	2.8800344	12
Pond 4	26-30 A	230	6	1000	770	80 0.1437662	2675.03	2797	67.666	-4.901	-5.4406667	0.0001308	5.4777825	28
Pond 4	0-4 B	410	2	1000	590	80 0.1111864	2074.446	1777	45.653	-2.218	-2.7576667	8.83142E-05	1.5886792	2
Pond 4	10-14 B	400	6	1000	600	50 0.1678231	2756.55	1938	50.269	-3.097	-3.6366667	9.72437E-05	2.917312	12
Pond 4	26-30 B	260	6	1000	740	80 0.1686865	3146.54	2650	65.119	-4.216	-4.7556667	0.0001259	4.4616454	28
Pond 4	0-4 C	500	2	1000	500	80 0.16	2985.179	1182	31.447	-1.526	-2.0656667	6.08332E-05	0.7604148	2
Pond 4	10-14 C	400	6	1000	600	50 0.2	3731.473	1957	49.063	-3.389	-3.9386667	9.48108E-05	2.8473231	12
Pond 4	26-30 C	350	6	1000	650	50 0.1615384	3013.882	1950	49.516	-3.96	-4.4986667	9.57871E-05	3.5576086	28
Pond 6	0-4 A	460	2	1000	520	80 0.1478231	2756.55	2948	61.217	-8.959	-8.9356667	0.0001786	2.4228946	2
Pond 6	10-14 A	380	6	1000	620	50 0.1838709	3430.548	4936	104.74	-8.957	-8.9336667	0.0002784	9.0012012	12
Pond 6	26-30 A	130	6	1000	870	80 0.0717241	1338.184	721	17.597	-10.501	-10.477667	4.66335E-05	3.8927087	28
Pond 6	0-4 B	500	2	1000	500	80 0.16	2985.179	3559	80.734	-9.353	-9.3296667	0.0002142	2.6786532	2
Pond 6	10-14 B	500	6	1000	500	40 0.24	4477.768	2793	63.747	-8.762	-8.7386667	0.0001705	4.2645148	12
Pond 6	26-30 B	320	6	1000	680	80 0.2258235	4214.37	1568	37.066	-9.369	-9.3456667	9.36852E-05	2.6452324	28
Pond 6	0-4 C	500	2	1000	500	80 0.16	2985.179	3079	66.886	-9.128	-9.1046667	0.0001803	2.2546598	2
Pond 6	10-14 C	500	6	1000	500	40 0.24	4477.768	2361	51.388	-9.466	-9.4726667	0.0001391	3.4768736	12
Pond 6	26-30 C	270	6	1000	730	80 0.1775342	3312.322	1027	22.783	-9.115	-9.0916667	6.21748E-05	2.1012782	28
Marsh	0-4 A	460	2	1000	540	80 0.1537254	2868.113	4609	108.871	-3.709	-3.9576667	0.0001683	2.1907131	2
Marsh	10-14 A	500	6	1000	510	40 0.24	4477.768	1895	43.966	-5.246	-5.2226667	0.0001000	2.501654	12
Marsh	26-30 A	400	6	1000	600	80 0.24	4477.768	3250	77.873	-5.788	-5.7646667	0.0001828	4.5711451	28
Marsh	0-4 B	470	2	1000	530	80 0.1418868	2647.234	3509	83.429	-4.412	-4.3886667	0.0002013	2.8388492	2
Marsh	10-14 B	400	6	1000	600	50 0.2	3731.473	1964	41.894	-5.19	-5.1666667	0.0001014	3.1244542	12
Marsh	26-30 B	400	6	1000	510	40 0.2309824	4302.169	2134	50.881	-5.653	-5.6296667	0.0001335	3.4740307	28
Marsh	0-4 C	500	2	1000	500	80 0.16	2985.179	4123	95.653	-3.71	-3.6866667	0.0002573	3.2163321	2
Marsh	10-14 C	360	6	1000	640	50 0.16875	3148.431	1567	36.847	-5.15	-5.1266667	0.0001004	3.8545368	12
Marsh	26-30 C	390	6	1000	610	50 0.1918033	3578.544	1888	42.984	-5.929	-5.9056667	0.0001256	4.0527078	28
greenhouse	A 0-4	405	2	1000	595	80 0.1080756	2031.928	886	20.081	-5.635	-5.6316667	5.48998E-05	1.0100278	2
greenhouse	A 10-14	470	6	1000	530	40 0.2128019	3970.851	1601	34.419	-4.119	-4.0956667	9.46419E-05	2.6680968	12
greenhouse	A 26-30	340	6	1000	660	40 0.1236636	2306.729	1453	33.804	-4.855	-4.8316667	9.33139E-05	4.5286777	28
greenhouse	B 0-4	380	2	1000	620	80 0.0980452	1829.626	564	13.034	-5.561	-5.5376667	3.62619E-05	0.7395517	2
greenhouse	B 10-14	430	6	1000	570	40 0.1810263	3377.965	1638	36.597	-3.045	-3.0216667	0.0001022	3.3872502	12
greenhouse	B 26-30	500	6	1000	500	40 0.24	4477.768	1671	37.468	-4.104	-4.0806667	0.0001050	2.6255024	28
greenhouse	C 0-4	310	2	1000	690	80 0.0718966	1341.167	488	11.208	-5.468	-5.4446667	3.23922E-05	0.9009508	2
greenhouse	C 10-14	300	2	1000	700	60 0.1542857	2878.565	1325	30.01	-3.4	-3.3766667	8.7056E-05	3.3855114	12
greenhouse	C 26-30	350	6	1000	650	50 0.1615384	3013.882	1336	30.01	-4.393	-4.3696667	8.73801E-05	3.2454703	28

POM data. Raw POM data from the MU IRMS lab.

Sample	Width(mm)	Carbon(mA)	Amplitude 44 (mV)	Area (Vs)	δ13C vs PDB	%Carbon	mg Carbon	Depth	%C of bulk sample	Inbornator N peak area	Inbornator C peak area	calculated N	C/N from Inbornator	%N Inbornator
Pod 1 D-4 A	5.513	1.344511394	4567	206.58	-7.274	24.3880	1.3151	2	27.751	bad baseline	352801	690802.16	0.1215899917	6.7519	4.3474
Pod 1 D-4 B 2	3.225	0.819476267	3112	125.033	-7.084	25.4101	1.8061	2	28.822	bad baseline	bad base line				
Pod 1 D-4 B 1	3.449	0.908117069	2313	121.088	-6.945	26.3314	0.8736	2	29.202						
Pod 1 D-4 C 2	3.048	0.824838232	3137	125.859	-6.8	27.0616	0.8114	2	29.251		344434	704958	0.1168233509	6.9727	4.2834
Pod 1 D-4 C 1	3.202	0.92051865	2356	122.742	-6.534	28.7480	0.8855	2	30.385						
Pod 1 10-14 A	7.141	0.806922217	3044	125.094	-8.721	11.2998	0.7936	12	13.770		322931	703163.9	0.1065672866	8.6115	1.8491
Pod 1 10-14 B	3.569	0.304285388	1241	45.926	-9.384	8.5258	0.2961	12	10.545		102370	256812.4	0.1036823917	8.3205	1.3114
Pod 1 10-14 C	5.408	0.366582837	1500	57.133	-9.703	6.7654	0.3587	12	8.394	bad baseline	bad base line				
Pod 1 10-14 C1	3.146	0.217138178	1268	47.725	-9.665	6.9020	0.2132	12	8.578						
Pod 1 26-30 A2	3.202	0.316164382	1235	45744	-10.539	9.6740	0.3077	28	11.767		102457	270742	0.0365684	8.7531	1.4093
Pod 1 26-30 A1	3.403	0.362824121	1687	73.184	-10.632	10.0742	0.3335	28	12.000						
Pod 1 26-30 B	4.836	0.469291427			-10.676	9.7041	0.4614	28	12.096	bad baseline	bad base line				
Pod 1 26-30 B1	2.296	0.208814604	569	27.853	-10.842	9.0947	0.2053	28	11.335						
Pod 1 26-30 C 2	3.731	0.321162238	1292	48.487	-10.788	8.8079	0.3127	28	10.980		103055	27 46202	0.0370612	8.8257	1.2304
Pod 1 26-30 C1	3.15	0.285543202	831	37.823	-10.436	9.0014	0.2767	28	10.882						
Pod 1 D-4 A2	3.752	0.888533825	3341	135.642	-11.323	23.6283	0.8745	2	26.455	bad baseline	bad base line				
Pod 1 D-4 A1	3.639	1.033211573	2527	137.583	-11.269	28.3103	0.9919	2	30.937						
Pod 1 D-4 B 2	3.405	0.708430217	2732	107.92	-10.244	20.8056	0.6958	2	22.732		265427	606174.1	0.0820081468	7.7538	3.0078
Pod 1 D-4 B1	3.093	0.623192835	1660	83.188	-10.245	20.1485	0.6019	2	21.690						
Pod 1 D-4 C	3.861	0.884560347	3398	136.932	-11.13	24.4346	0.8828	2	26.671		359707	759656.6	0.1273842232	7.0082	3.8484
Pod 1 10-14 A	3.606	0.415367627	1666	62.864	-10.477	11.5190	0.4053	12	12.935		147229	352709.1	0.0820242259	8.0507	1.9001
Pod 1 10-14 B	3.956	0.641683941	2521	97.656	-10.236	16.2205	0.6296	12	17.400		226061	543088.1	0.0787271023	8.1321	2.1795
Pod 1 10-14 C 2	3.332	0.408820236	1633	61.846	-10.708	12.2695	0.3988	12	14.111		148112	347458.2	0.0822323358	7.8751	1.8514
Pod 1 10-14 C1	3.183	0.427549666	1161	57.052	-10.563	13.4323	0.4146	12	15.366						
Pod 1 26-30 A2	3.227	0.530465451	2050	80.467	-11.222	16.4383	0.5190	28	17.955		194757	452434	0.0861234419	7.8458	2.3567
Pod 1 26-30 A1	3.8	0.668404002	1692	87.901	-11.146	17.3264	0.6357	28	18.677						
Pod 1 26-30 B 2	3.165	0.5315425	2090	80.677	-11.511	16.7944	0.5202	28	17.974		193305	454909	0.0903252233	7.7480	2.3054
Pod 1 26-30 B1	3.246	0.546902059	1459	72.967	-11.344	16.8362	0.5287	28	17.812						
Pod 1 26-30 C	3.035	0.427102925	1715	64.664	-11.339	14.0702	0.4188	28	15.396		145529	361173.6	0.0514481418	8.3200	1.6092
Pod 1 D-4 A	7.256	0.516242383	2051	80.523	-13.405	7.1147	0.5083	2	7.872		226158	561392	0.0754834476	7.8737	1.1981
Pod 1 D-4 B	7.797	0.568369407	2266	86.61	-13.663	7.3024	0.5584	2	7.714		197556	483851	0.0860711524	8.2441	0.9541
Pod 1 D-4 B1	7.209	0.567530059		88437	-13.101	7.7754	0.5590	2	8.818						
Pod 1 D-4 C	3.895	0.111959453	453	16.826	-11.233	3.0300	0.1098	12	3.418		34931	93807	0.0133855558	7.6322	1.3445
Pod 1 10-14 A	6.878	0.858162344	3231	133.141	-13.538	12.4769	0.8451	12	8.459		364799	748750	0.1200111101	8.3128	0.4403
Pod 1 10-14 B	5.376	0.428155666	1728	66.828	-11.57	7.9642	0.4207	12	9.353	bad baseline	bad base line				
Pod 1 10-14 C	3.727	0.208117626	792	36.004	-11.802	7.2269	0.2637	12	8.451						
Pod 1 10-14 C1	6.256	0.68035195		107.374	-13.623	11.3985	0.6802	28	12.600		242237	606498	0.0812366642	9.7320	1.3063
Pod 1 26-30 A	6.466	0.742322535	2663	115.374	-13.613	11.4804	0.7314	28	12.726		270204	648882	0.0886366646	9.4444	1.5996
Pod 1 26-30 C 2	3.702	0.367885946	1470	55.621	-13.076	9.6321	0.3566	28	10.956		119677	312978	0.0427393316	8.6960	1.3062
Pod 1 26-30 B	3.734	0.413226081	1121	55.193	-12.717	11.0666	0.4013	28	12.153						
Pod 1 26-30 C1	4.976	0.579986634	2305	88.148	-9.477	11.6569	0.5683	2	14.416		217464	491220	0.0756814961	7.6468	1.9231
Pod 1 D-4 A1	3.366	0.187380784	566	24.987	-10.234	5.5689	0.1847	2	6.927						
Pod 1 D-4 B 2	3.883	0.304175114	1231	45.899	-10.649	8.2589	0.2980	2	10.406		113796	250859	0.0406899469	7.5629	1.4312
Pod 1 D-4 C	6.786	0.666137174	2534	100.47	-10.417	9.9216	0.6360	2	12.033	bad baseline	bad base line				
Pod 1 D-4 C1	3.201	0.312100242	874	41.714	-10.161	9.7688	0.3046	2	12.216						
Pod 1 D-4 B1	3.513	0.312727137	883	41.722	-10.856	8.9020	0.3047	2	11.233						
Pod 1 10-14 A	30.857	0.622235324		96.799	-11.157	2.0165	0.6125	12	2.356		202618	540193	0.0870347782	10.4235	0.2813
Pod 1 10-14 B 1	27.092	1.112908884	4034	171.721	-10.936	4.1079	1.0920	12	5.013	bad baseline	bad base line				
Pod 1 10-14 B1	3.643	0.132223993	379	17.371	-11.25	3.5746	0.1301	12	4.442						
Pod 1 10-14 C	25.688	0.992039791	3635	153.51	-10.926	3.8654	0.9755	12	4.484	bad baseline	bad base line				
Pod 1 26-30 A1	28.835	0.777436693	3009	118.648	-11.609	2.6962	0.7649	28	3.211		229430	667650	0.0799883204	9.7481	0.3352
Pod 1 26-30 A2	34.834	0.67594 1578	2646	104.994	-11.67	1.9405	0.6650	28	2.310	bad baseline	bad base line				
Pod 1 26-30 A1	3.224	0.05509185	170	7.351	-12.35	1.7035	0.0583	28	2.182						
Pod 1 26-30 B P	27.646	0.700165362		106.862	-11.762	2.2346	0.6896	28	3.103	bad baseline	bad base line				
Pod 1 26-30 B 2	27.423	1.0472 39067		161.737	-11.63	3.8188	1.0281	28	4.662	bad baseline	bad base line				
Pod 1 26-30 B 2 ?	27.42	1.163215224		179.321	-10.999	4.2422	1.1407	28	5.173	bad baseline	bad base line				
Pod 1 26-30 B1	3.512	0.088673851	267	11.832	-12.059	2.5249	0.0904	28	3.185						
Pod 1 26-30 C 1	30.544	0.329239652		45.715	-11.853	0.9570	0.2956	28	1.092		93931	256277.55	0.0330353386	10.1547	0.1252
Pod 1 26-30 C 2	32.144	0.354792164		55.43	-11.855	1.1038	0.3478	28	1.252		123060	315397.28	0.0423887108	9.6336	0.1526
Pod 1 26-30 C1	3.074	0.031251704	90	4.171	-13.444	1.0196	0.0355	28	1.337						

Methane data. Raw data from the UNC IRMS lab. Data marked "corrected" had the baseline remarked manually. This was done because the computer had trouble resolving the methane peak on the chromatogram from the carbon dioxide peak for some samples. The baselines were reevaluated for all samples for the sake of consistency.

sample	spec #	peak amplitude	peak area	background 45	δ13C (computer)	corrected area	corrected background	corrected δ13C	depth
greenhouse 0-4 A (1)	42403	0.114	0.722	258.66	-100.98	0.767	252.36	-65.8	2
greenhouse 0-4 B (1)	42416	0.182	1.04	252.42	-73.27	1.03	253.16	-72.64	2
greenhouse 0-4 C (1)	42424	0.129	0.725	256.75	-69	0.782	252.36	-66.49	2
greenhouse 10-14 A (1)	42402	0.273	1.798	252.46	-70.69	1.814	252.22	-70.43	12
greenhouse 10-14 B (1)	42415	0.08	0.434	256.6	-74.63	0.478	252.41	-67.43	12
greenhouse 10-14 C (1)	42418	0.207	1.204	254.49	-70.58	1.186	255.84	-70.34	12
greenhouse 26-30 A (1)	42401	0.326	2.156	252.42	-67.08	2.16	253.07	-66.83	28
greenhouse 26-30 B (1)	42414	0.309	1.65	266.16	-64.79	1.839	254.41	-64.67	28
greenhouse 26-30 C (1)	42427	0.268	1.596	256.07	-68.53	1..622	254.04	-66.36	28
greenhouse 0-4 A (2)	42413	0.371	2.039	267.13	-59.21	2.245	254.21	-61.43	2
greenhouse 0-4 B (2)	42428	0.232	1.325	262.08	-64.08	1.453	253.09	-64.02	2
greenhouse 0-4 C (2)	42417	0.192	1.113	252.37	-63.39	1.107	252.87	-63.23	2
greenhouse 10-14 A (2)	42412	0.411	2.436	257.55	-73.53	2.491	254.36	-74.06	12
greenhouse 10-14 B (2)	42423	0.339	1.815	267.06	-61.06	2.025	253.37	-60.78	12
greenhouse 10-14 C (2)	42429	0.288	1.723	253.88	-72.57	1.731	253.24	-71.64	12
greenhouse 26-30 A (2)	42411	0.396	2.38	263.37	-66.74	2.531	254.31	-67.4	28
greenhouse 26-30 B (2)	42419	0.313	1.696	266.93	-58.72	1.889	253.89	-57.68	28
greenhouse 26-30 C (2)	42426								28
Pond 1 0-4A	42474	0.317	1.581	264.49	-51.39	1.752	253.68	-52.19	2
Pond 1 0-4B	42463	0.193	0.999	263.41	-55.83	1.098	255.53	-55.56	2
Pond 1 0-4C	42480	0.343	1.625	273	-52.3	1.901	254.16	-52.64	2
Pond 1 10-14A	42475	0.271	1.396	261.82	-59.94	1.506	254.03	-60.17	12
Pond 1 10-14B	42482	0.308	1.413	278.62	-60.13	1.76	254.1	-59.18	12
Pond 1 10-14C	42435	0.324	1.716	261.56	-56.34	1.818	254.58	-55.8	12
Pond 1 26-30A	42462	0.241	1.265	263.59	-60.07	1.401	253.93	-59.22	28
Pond 1 26-30B	42454	0.376	1.939	262.66	-57.32	2.049	255.54	-56.53	28
Pond 1 26-30C	42458	0.239	1.252	265.48	-56.63	1.336	258.86	-57.41	28
Pond 4 0-4A	42473	0.278	1.454	252.95	-72.16	1.452	253.05	-71.84	2
Pond 4 0-4B	42470	0.294	1.565	254.65	-73.53	1.54	256.24	-73.56	2
Pond 4 0-4C	42452	0.397	2.169	253.31	-73	2.16	253.78	-72.27	2
Pond 4 10-14A	42455	0.297	1.412	271.24	-72.33	1.67	253.74	-72.67	12
Pond 4 10-14B	42476	0.155	0.787	258.58	-74.95	0.857	252.86	-72.95	12
Pond 4 10-14C									
Pond 4 26-30A	42448	0.347	1.82	259.71	-69.07	2.028	253.68	-73.17	28
Pond 4 26-30B	42449	0.168	0.854	264.2	-76.14	0.998	252.98	-74.31	28
Pond 4 26-30C	42466	0.352	1.783	264.08	-76	1.947	253.46	-74.91	28
Pond 6 0-4A	42459	0.289	1.527	261.58	-49.46	1.664	253.97	-48.21	2
Pond 6 0-4B	42456	0.371	1.848	269.55	-51.77	2.112	253.65	-51.39	2
Pond 6 0-4C	42431	0.461	1.866	321.91	-51.25	3.019	253.52	-51.16	2
Pond 6 10-14A	42425	0.314	1.754	269.33	-52.42	1.992	253.3	-51.15	12
Pond 6 10-14B	42450	0.507	2.709	268.59	-51.36	2.955	253.87	-51.65	12
Pond 6 10-14C	42465	0.779	3.841	281.68	-52.66	4.375	253.47	-52.63	12
Pond 6 26-30A	42461	0.412	2.153	271.12	-51.12	2.421	254.1	-50.99	28
Pond 6 26-30B	42464	0.351	1.865	263.06	-49.74	2.009	253.6	-49.79	28
Pond 6 26-30C	42433	0.548	2.803	290.31	-48.17	3.428	253.84	-48.06	28
Marsh 0-4A	42451	0.186	1.006	256.24	-60.03	1.06	252.82	-58.19	2
Marsh 0-4B	42481	0.234	1.254	252.48	-60.28	1.234	254	-60.73	2
Marsh 0-4C	42436	0.157	0.868	254.01	-60.72	0.868	254.02	-60.37	2
Marsh 10-14A	42460	0.272	1.435	254.77	-62.89	1.444	254.09	-62.25	12
Marsh 10-14B	42479	0.247	1.319	253.23	-64.52	1.304	254.28	-63.94	12
Marsh 10-14C	42468	0.192	1.009	255.15	-63.5	1.028	253.69	-63.47	12
Marsh 26-30A	42439								28
Marsh 26-30B	42438	0.155	0.664	275.73	-56.94	0.947	253.19	-59.28	28
Marsh 26-30C	42453	0.141	0.79	253.51	-60.92	0.787	253.78	-60.78	28